IEEE Access
Multidisciplinary | Rapid Review | Open Access Journal

Received June 15, 2021, accepted June 25, 2021, date of publication July 1, 2021, date of current version July 13, 2021.

Digital Object Identifier 10.1109/ACCESS.2021.3094027

Memristor Fabrication Through Printing Technologies: A Review

SHAWKAT ALI[1,2], SALEEM KHAN[1], ARSHAD KHAN[1], AND AMINE BERMAK[1], (Fellow, IEEE)

[1]Division of Information and Computing Technology, College of Science and Engineering, Hamad Bin Khalifa University, Qatar Foundation, Doha, Qatar
[2]Department of Electrical Engineering, National University of Computer and Emerging Sciences (FAST NUCES), Islamabad 44000, Pakistan

Corresponding author: Shawkat Ali (shaali@hbku.edu.qa)

This work was supported by the National Priorities Research Program (NPRP) from the Qatar National Research Fund (a member of Qatar Foundation) under Grant NPRP11S-0110-180246.

ABSTRACT Memristor got a significant attraction to be the next generation memory device due to its small size, simple architecture, high density, and low power consumption. A memristor is a passive two-terminal primary electronic device with a built-in non-volatile memory function that can be fabricated in a crossbar structure. In the literature, independent studies have been reported on memristor manufacturing concerning the spatial resolution of the crossbar electrodes, and thickness of the active layer. However, this paper presents a comprehensive review different from others by comparing all the additive manufacturing technologies and their limitations for the development of a memristor array. A detailed study is performed about the pattern resolution, active layer fabrication, commonly used substrates, and device encapsulation methods. This review will provide a strong basis for the researchers, especially those working in the field of printed memristor devices.

INDEX TERMS Memristor, printing technologies, thin films, crossbar electrodes, memristor fabrication.

I. INTRODUCTION

Memristor was known with the name of resistive switch and extensively researched since 1960s [23], [24]. A crossbar resistive switch array was of great interest because of its simple structure and non-volatile properties. In 1972 Leon Chua postulated memristor as the fourth basic electronic element [38]. Since then it was a theoretical element that needed to be proven with some physical model. In 2008 HP lab demonstrated a resistive switch and they called it a first physical memristor [39]. Memristor was then became popular and researched worldwide, the popularity can be seen from the number of papers published since 2010 onward as shown in FIGURE 1. Memristor is a passive two terminals device composed of metal/dielectric/metal stacked structure. The physical operation mechanism relies on the formation and rupture of conductive filament (CF) with defects in the sandwich layer between the two metallic electrodes. For a virgin memristor an initial operation of electroforming usually required to generate the CF [40]. Some of the memristor devices do not require electroforming of CF due to the active layer and electrode material selection [41], [42]. After the CF formation, a memristor device can perform reversible switch between a high-resistance state (HRS) and a low-resistance state (LRS). The switching operation from HRS to LRS is called the set process. On the contrary, the switching operation from LRS to HRS is called the reset process. Memristor devices can be fabricated through a variety of fabrication technologies depending on the size, and target application of the device. Memristor size varies from nano-meter (nm) to micrometer (μm) depending on the technology used in the development of memristor [43]–[45]. Printed memristors are comparatively of large size i.e. in micrometer whereas, the solid state memristors are in nanometer size [19], [46]. As compared to solid state processing, printed electronics technology is a good option for the rapid prototyping of devices because of ambient processing, low cost, rapid fabrication and low material wastage [47]. These attractive features of the printed electronics have attracted researchers to explore new avenues for materials processing and to develop resistive switching devices on flexible, transparent, and stretchable substrates which otherwise

The associate editor coordinating the review of this manuscript and approving it for publication was Sun Junwei.

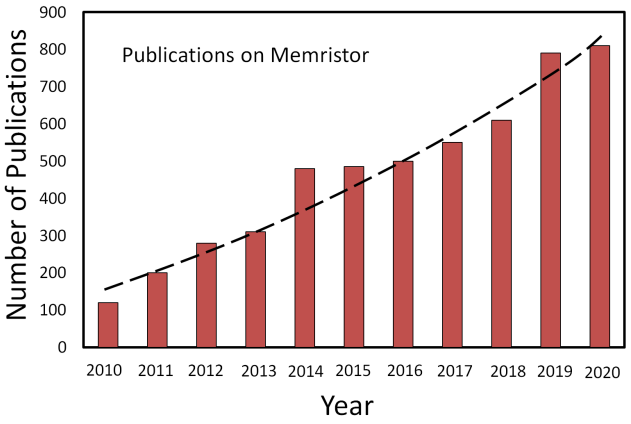

FIGURE 1. The number of publications on memristor technology from 2010 to 2020 [53].

are difficult to realize with the conventional cleanroom fabrication techniques [48], [49]. Traditional approaches for memristor device fabrication involves transferring the functional inks according to the pre-designed pattern of electrodes and active layer thin films on a substrate precisely. Various printed electronics fabrication technologies are available with certain limitations and advantages over the others. In order to achieve the target fabrication of memristor device, a specific fabrication technique, material, and procedure is adopted.

This paper presents a survey of various technologies used in printed memristor fabrication particularly resistive random-access memory (RRAM), conductive bridging rand-access memory (CBRAM), and metal oxide random-access memory (OxRAM). Till now there is no review article available dedicated to the printed memristors fabrication technologies; however individual articles are published on memristor fabrication through different printed electronics technologies. For example, inkjet printed memristor by Nelo *et al.* [19] focuses on inkjet printing process for the development of memristor, Paul *et al.* [50] focuses on spin coating technique, Sharma and Rabinal [51] have developed memristor through dip-coating, Patil *et al.* [52] have presented memristor fabrication through doctor blade coating, and Ali *et al.* [5] have discussed memristor fabrication through Electrohydrodynamic technique. This survey paper brings together various printing techniques used for the fabrication of printed memristors present in the literature till to date and provides a detailed discussion involving the key substrate materials, and encapsulation methods. This paper is organized as follows:

Section II presents memristor architecture. Section III presents memristor fabrication technologies, where various fabrication techniques are discussed. Section IV presents crossbar electrodes fabrication. A comprehensive survey of various process parameters, system and materials related requirements with illustrative examples of manufactured devices and circuits is also presented. Section V presents the active layer fabrication, challenges and suitable tools. Section VI presents challenges associated with top electrode fabrication, their possible solution and techniques. Section VII describes substrates for the memristor fabrication, their characteristics and applications. Section VIII presents details about the device encapsulation and techniques.

II. ARCHITECTURE OF A MEMRISTOR

Simple architecture makes it very interesting to research and rapid prototype the memristor devices. Memristor is a three layers device i.e. bottom electrode, sandwich layer, and top electrode [5]. Bottom and top electrodes can be of various metals and conductive polymers, whereas the sandwich layer can be a metal oxide, dielectric, insulator, or polymer. Memristor devices can be easily integrated to make an array of particular M $\times$ N size by placing the memristor cells in columns and rows as shown in FIGURE 2. Bottom electrodes are deposited on the substrate by using a suitable fabrication technique. Similarly active layer is deposited and then the top electrode as the cross-sectional view is shown in FIGURE 2. The attractive thing in the fabrication is that there is no need to deposit active layer separately for the individual device but a thin film covering the bottom electrodes [54]. The area under the overlap of bottom and top electrode acts as an active layer which is usually nanometer size. Due to enough spacing between devices i.e. $4F^2$ the crosstalk or charge leakage is negligible in the active layer which is shared by the array.

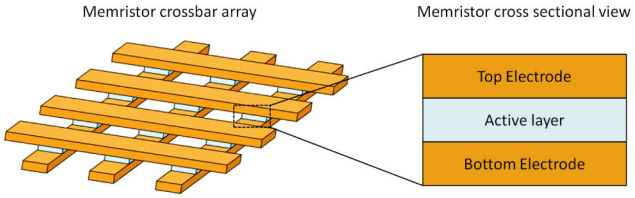

FIGURE 2. Memristor crossbar array and single cell architecture.

III. MEMRISTOR FABRICATION TECHNIQUES

Memristor is consisted of bottom and top metallic electrodes with sandwiched switching layer. Memristor size varies from nm to micrometer depending on the technology used in the development of memristor [55].

Commonly, the printed memristor are comparatively of large size i.e., in micrometer whereas, the solid state memristors are in nanometer size. Simpler memristor structure metal/insulator/metal enables a variety of fabrication technologies. On a target substrate bottom electrodes/switching layer/top electrodes are deposited by a suitable method with or without shadow mask technique. Bottom and top electrodes are commonly straight bars of nm to μm width, whereas the switching layer is nanometer thin film. Each layer is deposited and cured at appropriate temperature to achieve a good conductivity [56]. Memristor fabrication techniques are categorized as contact and non-contact processing as shown in FIGURE 3.

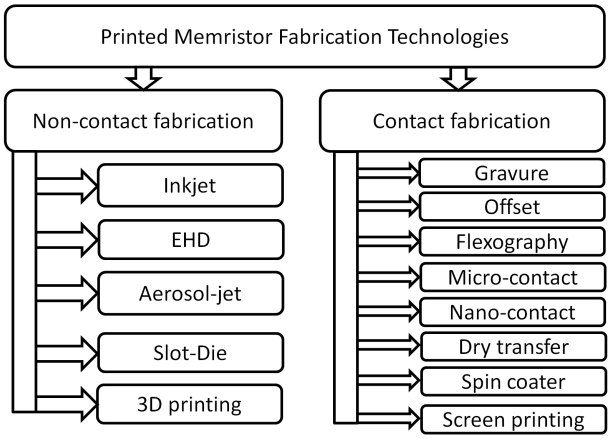

FIGURE 3. Classification of printing technologies for the memristor fabrication.

Solution processed technique is used for the memristor fabrication especially in the printed electronic domain [57], [58]. In this process various technologies can be used for the development of devices and circuits. Solution process can be applied on both organic and inorganic materials [59], [60]. The deposition techniques can be different according to the task; however, ultimate goal is the same to precisely deposit the material on the substrate. Nanoparticles or polymers can be dissolved in a suitable solvent. Solvent plays a role of carrier for the nano particle from the ink reservoir to the target substrate [61], [62]. The solution process-based deposition can be done with a variety of techniques which deposits the material according to the design i.e. patterns and thin films. Some of the solution processed methods of thin films and patterns fabrication, as shown in FIGURE 4. In all these techniques, ink is synthesized in a suitable range i.e. viscosity, surface tension, conductivity etc. Ink is deposited on the target substrate in the shape of patterns or thin films with the help of suitable technique. In the literature, memristors were developed through inkjet material printer [4], [63], Electrohydrodynamic printer [5], Sol-Gel spin coating [64], screen printing [65], dip coating [66], metering rod coating [67], aerosol-jet [68] doctor blade coating [69]. Solution processed techniques have their unique

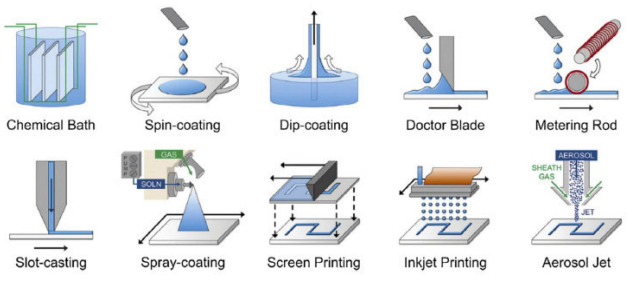

FIGURE 4. Solution processed techniques for the memristor fabrication [56].

properties and advantages over the others. Selection of the deposition technique is made on the basis of requirement i.e., pattern, thin film, thick film, or high aspect ratio patterns. For the memristor fabrication, these techniques can be adopted. These techniques can be divided into two categories for the memristor fabrication i.e., electrode fabrication, and active layer fabrication. Memristor requires patterning tools for the electrode fabrication with reasonable aspect ratio and width resolution. Memristor electrode fabrication techniques are explained in the below section.

IV. CROSSBAR ELECTRODES FABRICATION

Memristor is a combination of top/bottom electrodes and a sandwiched active layer between them. Memristor array uses crossbar electrodes as bottom and top metallic bars sandwiching the active layer. Electrode parameters such as width and thickness (height) can be controlled for the target application by adopting suitable fabrication technique. In terms of resistive switching mechanisms, memristors are two types of filament based and oxygen vacancy based. In the filament based memristor electrode parameters does not affect the performance of the memristor because a single filament (nanometer size) can switch the device from OFF to ON and vice versa. The filament is regardless of the electrode size in the filament based resistive switching device. However, in oxygen migration based memristors, electrodes width plays an important role in the base resistance of either state i.e. HRS and LRS, it was found that resistance decreases as the electrode width increases [70]. Electrodes can be fabricated through various techniques and materials. In printed electronics, usually non-conventional substrates are utilized for the fabrication of devices and circuits. A suitable technique according to the requirement can be adopted from a variety of printing techniques available for the memristor electrode fabrication. In the literature almost all the printing techniques are used for the memristor electrode fabrication. Prominent printing techniques for the memristor electrode fabrication are reviewed below.

A. INKJET MATERIAL PRINTER

Inkjet printing is a cost effective and direct patterning technique for solution-based materials deposition. Inkjet material printer deposits the material on the target substrate with the help of computer-controlled mechanism. A variety of commercially available materials and lab synthesized can be printed with inkjet material printer with appropriate viscosity [58], [71]. Inkjet printer generates droplets at high frequency and deposits on a moving substrate. The target circuit is designed through computer program and loaded into the printer along with material and substrate [72]. Inkjet printers mainly operate in two mechanisms, piezoelectric and thermal [73], [74]. In piezoelectric method the droplet is generated through a vibration of piezo crystal inside the nozzle head whereas, in the thermal inkjet technique a bubble is generated in the nozzle head through applied voltage to generate a droplet. (b) shows inkjet material printer in action,

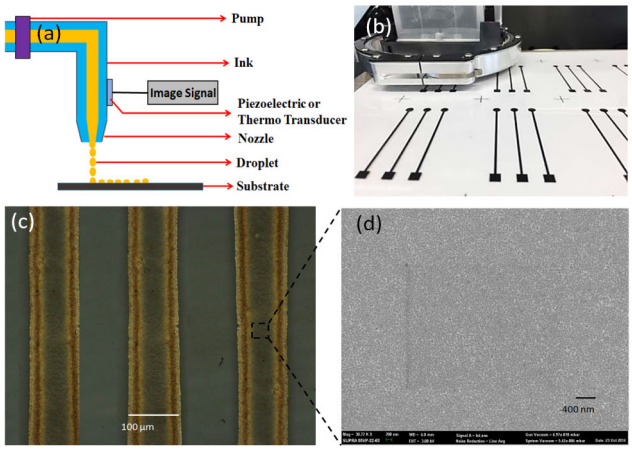

FIGURE 5. (a) inkjet printer schematic diagram, (b) inkjet printed memristor bottom electrodes, (c) microscopic image of memristor electrodes, (d) SEM image of printed silver electrode.

printing Schematic diagram of the inkjet material printer is shown in FIGURE 5(a), the system is composed of ink cartridge usually 3mL, nozzle head 16 to 125 nozzles in a row, computer-controlled platen with vacuum and heat options, and jetting control parameters drop frequency, wave shape and number of nozzles. The inkjet printer parameters can be tuned to achieve the target output in term of line width, thickness and fabrication speed. The inkjet printer can print the line width 15 to 100 μm and thickness of 0.01 to 0.5 μm depending on the material's viscosity, substrate treatment and drop spacing. FIGURE 5memristor bottom electrode bars. The image shows a 16 nozzles head printing in parallel; higher the number of nozzle speedy is the printing process. However, it is difficult to tune the entire nozzles uniformly to achieve synchronous droplets. Therefore, it is found that lower number of nozzles give a precise printing results as compared to high number of nozzles. Substrate treatment is very important for the inkjet printing to get uniform lines and strong adhesion. Usually untreated or wrongly treated substrate results in ink spreading or uneven line patterns which make circuit short or open circuit problems specially in small pitch patterns [75]. Figure 5(c) shows microscopic image of the inkjet printed silver material on the PI substrate, the results show a uniform and continuous line track as the substrate is well treated and printing parameters are tuned properly. With optimum printing parameters and treated substrate enables the repeatability of the printing process and improve the variability line to line. In memristor array, cell to cell variability is very important which is partially dependent on the electrodes as well as on the active layer film. Uniform electrodes make sure the line resistance to be fixed in each cell of crossbar array that can be compensated in both HRS and LRS states. If the crossbar electrode lines are not uniform in terms of line width and thickness (height) it can produce resistance and result in voltage drop that lead to variation in the memristor threshold voltage. Hence, non-uniform electrodes contribute in cell-to-cell variability and overall performance of the array. FIGURE 5(d) shows SEM image of the silver electrode. Other than the line width and thickness, the surface morphology is very important for the memristor performance. If the bottom electrode is not uniform in thickness, it can affect the active layer thickness and create variation in resistance and threshold voltage. Several results-based inkjet material printers have reported for the fabrication of memristor by utilizing different materials for the electrodes and active layer. An electrically generated memristor was reported in [76]. They reported a memristor composed of silver material only. They printed an hourglass-shaped silver pattern that is oxidized in the bottleneck region due to joule heating-induced by applying a high current to the device. In this design there is no sandwich active layer, rather it is a planar structure with a narrow bottleneck in the middle of line. [77] reported inkjet printed memristor device based on ITO/GO/Ag structure, they diluted the graphene oxide (GO) ink in distilled water and ethanol to achieve low viscosity of 2.2 cp. Inkjet assisted memristor was fabricated by using TiO2 active layer and gold electrode [78]. They used a planar substrate coated with gold, a narrow trench (∼700 nm) was developed with AFM and TiO2 ink was filled in the trench with inkjet printing to get a planar memristor as Gold/TiO2/Gold.

Inkjet material printers are available in different models according to their specifications such as desktop, standalone, number of print heads, number of nozzles, speed etc. A specific inkjet material printer can be chosen according to the requirement, mostly in academia and research work DMP 2850 is used. They are not heavy duty but very good option for the rapid prototyping. On the other hand, standalone systems such as DMP 3000 are used for the bulk production in the industry.

B. AEROSOL JET TECHNIQUE

Aerosol jet printing is modern and advanced additive fabrication technology that covers a wide variety of materials ranging from 1–1000 cP viscosity [79]. Aerosol systems provide high resolution as ∼10 μm and wide as mm range, which makes it attractive for printed electronics fabrication including patterns and films. The principle of operation is based on the droplets generation of the functional materials through pressure of sheath gases [80]. The material can be atomized through two different techniques, ultrasonic, and pneumatic as shown in FIGURE 6 (a, b). In pneumatic atomizer aerosol jet is generated by applying gas/air in the ink chamber through a tube. With the supplied gas/air, the ink level in the chamber rises and reaches the middle hole of the tube as shown in the figure. The excessive ink is ejected through the hole with applied pressure which converts into micro droplets. In addition to this process, an exhaust tube is taken out to a reservoir where excessive mist is stored. After the exhaust tube, dense mist is directed towards the nozzle head through virtual impactor. Sheath gas is applied to the nozzle to concentrate the micro droplets and eject from

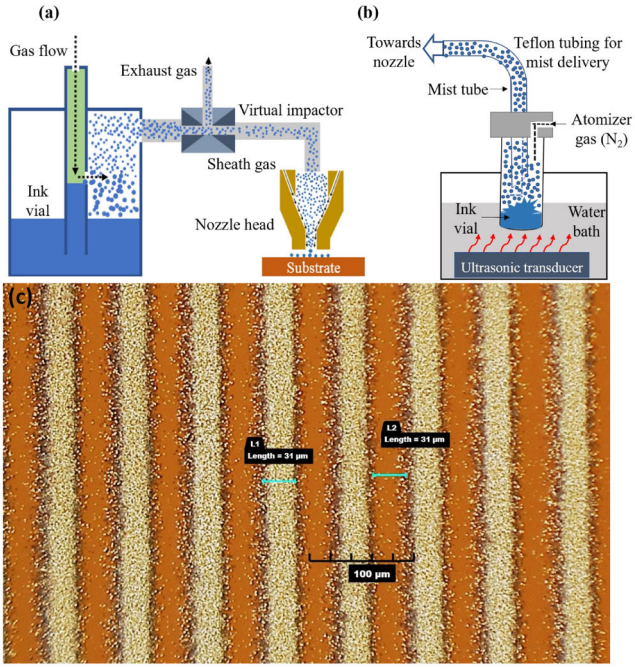

FIGURE 6. Schematic diagram of aerosol jet printing process (a) pneumatic, (b) ultrasonic, (c) Bar electrodes printed on PI substrate through pneumatic aerosol system [80].

the nozzle. The stream of droplets is ejected in the form of an intact jet, eventually deposited on the target substrate. The other type of aerosol is ultrasonic aerosol jet which is used for the high resolution patterning, especially metallic patterns. Ultrasonic aerosol can be manipulated to print wide lines in mm range. Ink atomization is achieved through pressure waves generated by ultrasonic actuator placed in a water tub containing the ink reservoir as shown in FIGURE 6(b). Atomizer gas (N_2) is applied to mix with the droplets generated through ultrasonication process. The mist is supplied to the nozzle through Teflon pipe. Another gas (sheath gas) is applied to the nozzle to concentrate the mist and make aerosol jet. The aerosol jet material is eventually deposited on the target substrate. FIGURE 6(c) shows bar electrodes printed on PI substrate by utilizing Au ink. Both aerosol systems offer a variety of advantages over the other printing techniques. High resolution patterns are used in miniaturized devices to improve head over and power consumption. The aerosol offers fine patterning as low as 10 μm thin which are highly conductive. In many gas sensors a heater is needed to reset the gas sensor, in this scenario aerosol printer plays an important role to fabricate micro-heaters which are small in size and draw very less power, suitable for localized heating system. Aerosol printed Au nanoparticle-based micro-heater was presented, effective area 150 $\times$ 150 μm2, power consumption of 22 mW and generated 250°C temperature [80]. Interdigital electrodes were printed with aerosol jet for the gas sensors in combination with inkjet printed sensing layer [81], [82]. The resolution of aerosol jet printer can be efficiently utilized in the memristor array fabrication for large integration. Memristor array fabricated through aerosol jet was demonstrated by utilizing Ag/MoS2/Ag [83]. Aerosol jet can be modified to deposit thin film for the memristor active layer of nm thickness.

Various aerosol jet systems are available in the market based on the principles of pneumatic atomizer aerosol jet and ultrasonic atomizer aerosol jet. Equipment can be different based on their specifications, and utilization such as resolution, speed, and number of nozzles. However, the operation principle is the same. Commonly used aerosol systems are OPTOMEC aerosol jet and integrated deposition solutions (IDS) Nanojet systems.

C. ELECTROHYDRODYNAMIC TECHNIQUE

Electrohydrodynamic technic is used to deposit patterns and thin films on various substrates. EHD system works on the principle of electric field that ionizes ink and makes a canonical jet. EHD system is usually consisted of ink reservoir, ink pump, nozzle, high voltage supply, moveable computer-controlled platen, and high-speed camera to monitor the spray. EHD is divided into two categories as continuous EHD and drop-on-demand EHD. Continuous EHD rapidly deposits the material on the target substrate regardless of the platen movement this mode is less efficient for the material saving. On the other hand, DOD EHD system ejects the ink in the form of small droplets controlled by a pulsating high voltage. DOD system can be control by pulsating DC voltage according to the requirement and circuit design. EHD system is shown in FIGURE 7(a), continuous and DOD system. EHD system can be operating at room temperature and open air. FIGURE 7(b) shows the EHD nozzle during printing, the ink is ejected from the nozzle with high speed, a controlled platen is required to move the substrate according to the circuit design, in case of memristor bottom electrodes a straight bar. EHD technique for the memristor fabrication is well reported in the literature. [84] Reported inkjet printed memristor based on silver electrodes on PET substrate and

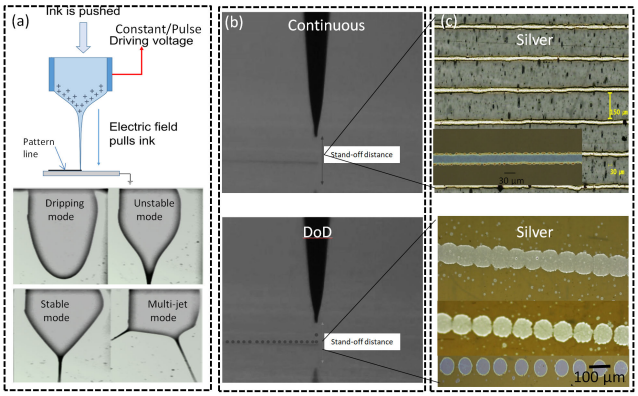

FIGURE 7. (a) Schematic diagram of the EHD system, continuous, and DOD [85], Dripping mode, unstable jet mode, Stable cone jet, Multi jet mode [7] (b) EHD nozzle in action continuous and DoD, (c) EHD printed patterns with continuous and DOD.

TiO_x sandwich layer. Memristor device based on ZrO_2 active layer and silver electrodes [5]. Electrodes were fabricated through continuous EHD system with line width of 100 μm and thickness of 500 nm.

D. SCREEN PRINTING TECHNIQUE

Screen printing technique is one of the most worldwide famous and old methods for the fabrication of printed electronic devices and circuits on various substrates. It is faster and more versatile in comparison to other printing tools, as it adds simplicity, affordability, speed and adaptability to the fabrication process. The results from screen-printing can be reproduced by repeating a few steps and an optimum operating envelope can be developed quickly [80]–[86], [86], [87], [87], [88], [88], [89], [89]–[91]. Screen printers are divided in to two main types and both can be used on R2R system, flatbed system and rotary system [86]. Screen printer is very simple as compared to other printing techniques, it is consisted of screen, squeegee, press bed, and substrate, as shown in FIGURE 8(a). In the flatbed system, the functional material poured on the screen front side and squeegeed to spread across the screen. This action transfers the material onto the substrate according to the screen pattern. Flatbed system is comparatively small and a good option for the prototyping and system optimization such as material and screen. On the other hand, rotary screen is bulky and used for mass production, in this system the squeegee and ink are placed inside the tube which is rotating over the substrate against the impression cylinder. Rotary system offer high fabrication speed as compared to flatbed but the drawback is costly screen and difficult to clean the screen [86], [92]. In both the systems, print quality is affected by various factors such as solution's viscosity, printing speed, angle and geometry of the squeegee, snap off between screen and substrate, mesh size and material [88], [93], [12]. FIGURE 8(b) shows a screen printer in action, a silver paste is loaded on the top of screen to spread over the entire patterned area of the screen with the help of squeegee. FIGURE 8(c,d) shows an SEM image of the screen printed silver bar electrodes with thickness of almost 100 μm. usually, printed memristors uses electrode width of minimum 100 μm to achieve good conductivity of the electrode line. If the line width is less, the resistance will increase and affect the device performance [94].

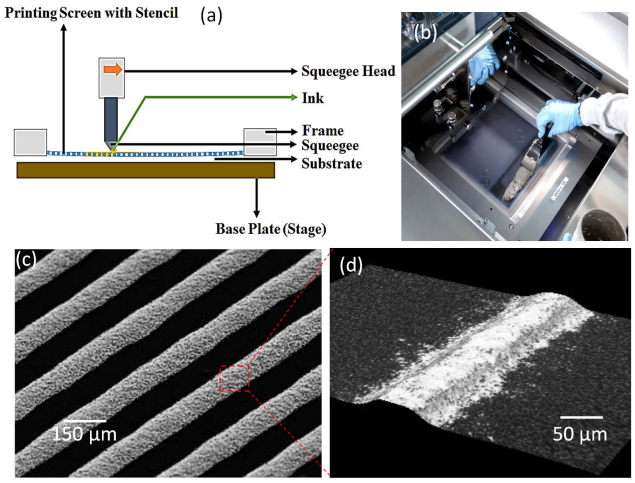

FIGURE 8. (a) schematic diagram of the screen printing setup, (b) loading screen printing silver paste for the lines printing, (c) screen printed silver lines can be used for bottom electrode [95], (d) 3D Nano profile image of the screen printed line [95].

Screen printing technique can be performed with various commercially available equipment such as fully automatic, semi-automatic, and manual. All screen printing machines follow the same protocol for the printing of a pattern or thin film as discussed above.

E. GRAVURE PRINTING

Gravure printing is one of the old and popular printing techniques used for the patterning on a variety of substrates. In the gravure printing process, the ink I filled onto the engraved cylinder, with the help of impression cylinder as shown in FIGURE 9(a). Gravure printing machine perform excess ink is removed with doctor blade; the engraved cylinder is brought in contact with the substrate direct transfer of functional inks in a single step through physical contact of the engraved structures with the target substrate. High quality and low-cost patterns can be produced with gravure system [92]. Usually, a low viscosity inks are used in the gravure printing when utilized in R2R system for mass production. The key component in a gravure printing machine is the large cylinder electroplated with copper material and microcells are engraved according to the pattern. The microcells holding pattern information are engraved through electromechanical procedure or by using a laser tool [86], [92], [96], [97]. Engraved cylinder is further chrome electroplated to prevent wear and tear during the ink transfer and contact with the substrate. During the printing operation, engraved cells are filled with the ink by using a reservoir beneath rotating gravure cylinder as shown in FIGURE 9(b). The engraved rotating cylinder picks up the ink from the reservoir; extra ink from the engraved cylinder is removed through a doctor blade. A pretreated substrate is moving with a certain speed between the engraved cylinder and impression cylinder. The main purpose of the impression cylinder is to put pressure on the substrate in order to keep it in physical-contact with the engraved cylinder. Functional ink from the engraved cylinder is transferred onto the substrate through capillary action. Surface properties of the substrate are treated with suitable process to maximize the transferability of the ink from the cells. Along with solution's properties such as viscosity and surface tension, engraved cell's width/depth ratio play a key role in the gravure printing process to achieve high speed of printing, as low viscosity ink allows the cells to empty rapidly once in contact with substrate [98]. Experimental results in the literature show that the ink transfer rate increases along with increment in the surface energy and contact angle [99]. Ratio of the engraved cells width/depth (approximately 7-8) is required for the better transfer of the ink onto the substrate [28].

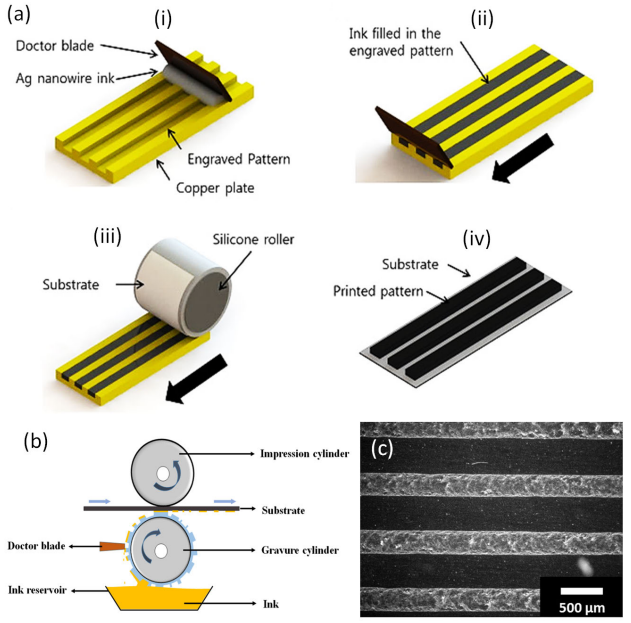

FIGURE 9. (a) A schematic diagram of the gravure printing process: (i) ink application, preparation for doctoring, (ii) doctored plate, (iii) printing by passing the filled pattern through nip of a plate roll set-up, and (iv) printed pattern on the substrate [100], (b) schematic diagram of the gravure printer, (c) silver micro-patterns printed through gravure printer [95].

The cells spacing ratio is also very important and usually it is in the range of 1.06-1.4 [28], results in a fairly uniform lines as shown in FIGURE 9(c). The cells size and spacing should be precisely matched, the acceptable tolerance in the cell size and spacing should be less than 1 μm. Acceptable features on gravure cylinder are required in terms of size and spacing which will not only insure suitable drop spacing but also an adequate cell emptying capability [28]. Donovan sung et. al presented gravure printed patterns with high resolution as 30 μm wide and 70 nm thick [28]. Yasuyuki et. al presented a highly conductive silver traces embedded in polycarbonate films [101].

F. FLEXOGRAPHY TECHNIQUE

Flexographic printing is very popular for its high-speed printing, high resolution patterns, and uses a wide variety of solutions and materials such as solvent-based, water-based, electron-beam curing inks, UV curing inks and two part chemically curing inks etc. Flexographic printer uses a rubber or polymer plate attached to a cylinder having raised patterns that are developed by photolithography and are [102]. FIGURE 10(a) shows flexographic printer schematic diagram, main components plate cylinder, printing plate, ink reservoir, anilox roller, and impression cylinder. Anilox cylinder picks the ink from the ink reservoir and transfer to the printing plate driven by plate cylinder. Printing plate transfers the image onto the substrate in combination with impression cylinder that pushes the flexible substrate towards the printing plate. Annilox roll primary controls the quantity of

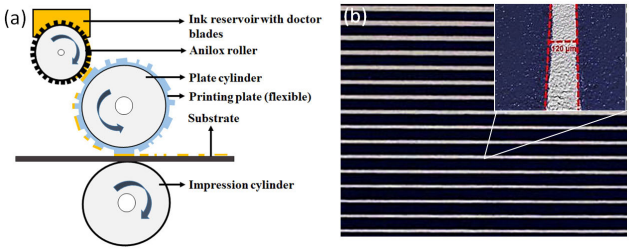

FIGURE 10. (a) flexographic printer schematic diagram, (b) flexographic silver lines printed on glass substrate [102].

ink to be transferred to the plate and to the substrate subsequently. As compared to gravure printing technique, flexographic technique provides high speed and high resolution with good repeatability. FIGURE 10(b) shows flexographic printed silver lines with various trace width [102]. In case of metallic inks, high concentrations of solutions are required for good conductivities and surface morphology, however the material viscosity should not be that high which do not fall into the operating envelope of typical flexographic printing [103]–[105]. Flexographic patterns with resolution between 50-100 μm are reported in literature and with proper control of process parameters and substrate surface properties; this could be reduced to around 20 μm with optimized parameters [105]–[107]. Flexographically printed films are reported to be uniform and slightly less smooth than the spin-coated/gravure printed films [108].

G. MICROCONTACT TECHNIQUE

Microcontact printing is a technique of transferring functional materials from patterned elastomeric stamp to a substrate. Targeted micro-patterned master is fabricated through photolithography, then a solution of poly(dimethylsiloxane) (PDMS) is casted on it to make a replica mold stamp. The PDMS stamp is then used to transfer the target solution material onto a substrate through conformable contact. For successful transfer of structures, a conformal contact of patterned elastomeric stamp with target surface is essential. Placement of the PDMS stamp on the substrate is also very important in order to achieve the transfer precisely. Main advantage of the micro-printing technique is to produce multiple copies of the pattern by using patterned stamp [32], [109]–[111]. As compared to other elastomers including, Polyimides, Polyurethanes, and cross-linked Novolac resin, PDMS is the best candidate. FIGURE 11(a) shows PDMS stamp preparation and ink transfer onto a substrate through PDMS stamp through microcontact printing technique. Micrometer patterns are generated in silicon substrate according to the design. Usually, computer controlled milling machine is used to develop silicon master. Standard photolithography is also used for high resolutions and complex structures by incorporating microfluidic channels [109], [111], [112]. PDMS material is then poured on the pattern, which takes the shape of the master and makes a soft flexible mold. It is cured at

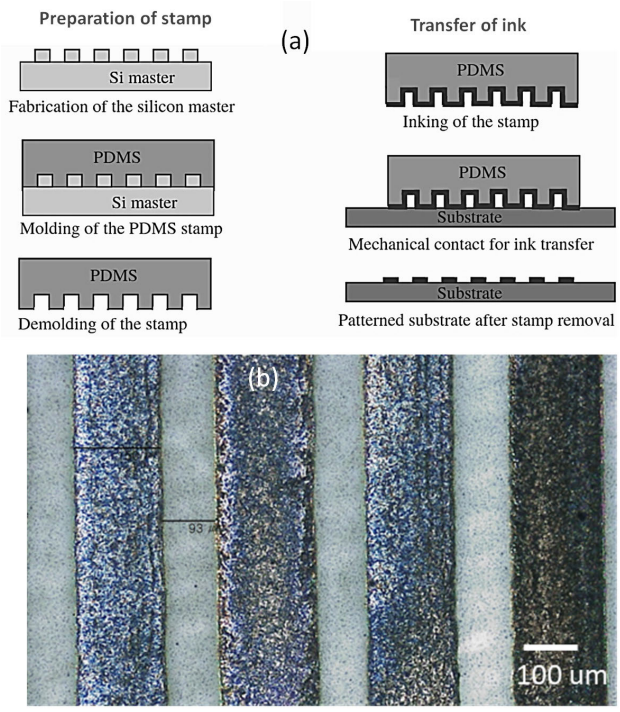

FIGURE 11. (a) Microcontact printing: PDMS stamp preparation and ink transfer onto substrate through stamp.

80 °C temperature in a lab furnace to polymerize the PDMS. After the polymerization of PDMS material, it is peel off from the silicon master. The PDMS mold is now ready to be used as a stamp, it is then fixed in a hard substrate in such a way that PDMS soft patterned face is exposed to be dipped in the ink. Similarly, the ink transfer through PDMS mold is shown in FIGURE 11(a). PDMS mold is dipped in the ink, it is then placed on the target substrate and pressed with appropriate pressure to make a conformable contact. The ink is transferred onto the substrate in the shape of patterns. FIGURE 11(b) shows a microcontact transferred silver bar electrode around 150 μm.

V. ACTIVE LAYER FABRICATION

The retention characteristics of the memristor to remember the last resistive state is due to the permanent displacement of charge within the device switching layer [113]. The switching layer can do the switching by either itself or in combination with bottom and top electrodes. In some models, the active layer can do switching independent of the electrodes such as in the HP model, where TiOx and TiO2. In this case, the oxygen vacancies from the TiOx moves to the TiO2 region and makes it conductive (ON), whereas by applying reverse polarity, the oxygen vacancies from the TiO2 region move back to TiOx and makes the device OFF [39]. In some models, the active region reacts with top electrode and makes an oxide layer at the interface [77], [114]. In this scenario, oxygen ion moves between the active layer and interface which perform the switching function. Charge trapping memory utilizes the active layer for the charge trapping, which makes conductive path for the current through the active layer [115], [116]. Another model is based on the electrochemical metallization, where metals from the electrodes penetrate into the active layer and make a conductive bridge between the electrodes [117], [118]. Several models are associated with the switching mechanism of memristor depending on the active layer material and electrodes. In all cases, an active layer is essential to perform the switching. An active layer with thickness of nanometer size can be deposited with a variety of printed electronics techniques. Depending on the active material, electrodes, and films thickness, a suitable active layer fabrication tool can be used. The detail technical comparison of the active layer fabrication tools is given in Table. 1. Most of the techniques discussed above can be efficiently utilized for the fabrication of memristor active layer. However, some fabrication tools such as screen printer, nano imprint etc. cannot be used for the active layer fabrication because they cannot deposit nano scale thickness of the film. The most efficient tools for the active layer fabrication are spin coater, ESD, and aerosol. In these tools, film thickness can be controlled through tuning the printing parameters. Some of the active layer fabrication techniques are given below in detail.

A. SPIN COATING TECHNIQUE

Spin coater is a very simple and cost-effective tool for the fabrication of thin films on various substrates. Spin coater is consisted of spinner, and electronic control unit to gt the required revolution per minute. FIGURE 12(a) shows a schematic diagram of the spin coater, main components are chuck, spinner, vacuum generator, and electronic control unit. Substrate is placed on the substrate holder, and vacuum generator helps to keep the substrate attached with substrate holder during spinning. Ink is poured with the help of a pipette either on a rotating substrate or stationary substrate according to the requirement. Ink spreads over the entire substrate due to centrifugal force during spinning. The thickness of the film is controlled through spinning speed and time. Usually, solvent is evaporated during the spinning time and material in the form of thin film is left on the substrate. FIGURE 12(b) shows a schematic diagram of the spin coating process steps. First step is deposition, when ink is poured over a substrate. In the first step, the ink is casted onto the substrate through a pipette on a rotating (dynamic spin coating) or stationary (static spin coating).

The centrifugal motion of the substrate holder spread the ink across the substrate. The substrate holder then reaches the target rotation speed, it can be immediately after the deposition of ink or following a lower speed spreading step called ramp. During this time, most of the ink material leaves the substrate due to high centrifugal force on it. In the ramp duration, the ink is spinning at a lower rate than the substrate, but gradually the rotation of ink increases and match with substrate speed when ink becomes level. At target RPM, the ink becomes thinner as it is dominated by centrifugal forces. When the excessive ink droplets stop leaving the substrate,

TABLE 1. Patterning and coating techniques for memristor fabrication.

S.No	Parameter	Inkjet	EHD	Aerosol jet	Screen printing	Flexographic	Spin-coater	Slot-die	Offset	Gravure	Nanoimprint	Transfer
1	Print Resolution (μm)	15-100	10-500	10-100	30-100	30-80	NA	200	20-50	50-200	1-20	4-50
2	Print Thickness (μm)	0.01-0.5	0.01-0.5	0.1-5	3-30	0.17-8	0.1 - 10	0.15-60	0.6-2	0.02-12	0.18-0.7	0.23-2.5
3	Printing Speed (m/min)	0.02-5	0.1-3	0.6-1.2	0.6-100	5-180	NA	0.6-5	0.6-15	8-100	0.006-0.6	NA
4	Req. Solution Viscosity (Pa. S)	0.001-0.10	0.001-0.10	1-1000	0.500–5	0.010-0.500	NA	0.002-5	5 – 2	0.01-1.1	~ 0.10	NA
5	Solution Surface Tension (mN/m)	15-25	15-25	10-15	38-47	13.9 -23	NA	65-70	NA	41- 44	22-80	NA
6	Material Wastage	No	No	No	Yes	Yes	yes	Yes	Yes	Yes	Yes	No
7	Controlled Environment	No	No	No	No	Yes	No	No	Yes	Yes	No	Yes
8	Experimental Approach	Contact-less	Contact-less	Contact-less	Contact	Contact	Contact	Contact-less	Contact	Contact	Contact	Contact
9	Process Mode (sample pattern line)	Single-Step	Single-Step	Single-Step	Multi-Steps	Multi-steps	single step	Single-Step	Multi-Steps	Multi-steps	Multi-steps	Multi-Steps
10	Mask Requirement	No	No	No	Yes	No	Yes	No	No	No	No	Yes
11	Printing area	Large	large	Large	Medium	Large	Medium	Large	Large	Large	Medium	Medium
12	Electrode fabrication	Yes	Yes	Yes	Yes	Yes	No	Yes	Yes	Yes	Yes	Yes
13	Active layer fabrication	Yes	Yes	Yes	No	Yes	Yes	Yes	No	No	No	Yes
14	References	[1-3]	[4-7]	[8-11]	[12-14]	[1, 15, 16]	[17-20]	[21, 22]	[25-27]	[1, 28-31]	[31-34]	[35-37]

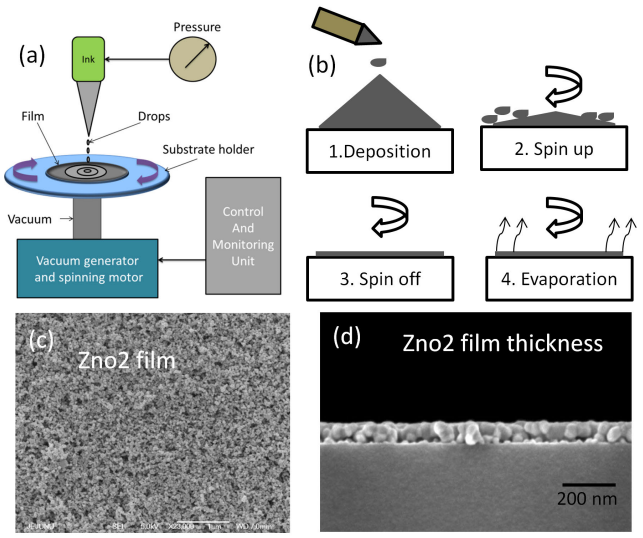

FIGURE 12. (a) Schematic diagram of a spin coater, (b) spin coating steps for the thin film fabrication, (c) SEM image of the ZnO2 spin coated film, (d) ZnO2 thin film cross sectional SEM image.

it indicates the film is thickness is finalized. Edge effects are sometimes seen because of two possible reasons, the ink viscosity is high, or the ink amount poured was not enough to cover the entire substrate, and the solvent is volatile that evaporates during the ramp or in the start of spinning period. Finally, ink droplets and spreading stops and film thinning is dominated by evaporation of the solvent. FIGURE 12(c) shows an SEM image of the ZnO2 thin film coated through spin cater at 1500 rpm for 2 min. FIGURE 12(d) shows a cross sectional SEM image of the ZnO2 active layer, it can be seen that the thickness is uniform, and the height is almost 100 nm throughout the area. Spin coated memristor was reported Ag/SP-GaOx/SP-AlOx/ITO [119]. The memristor exhibited 2 × 104 s retention time, 1000 endurance cycles, and 2 × 104 ON/OFF ratio. Spin coating systems are categorized on their specifications such as revolution per minute, ramp functions, substrate holding chuck size.

B. ELECTROSTATIC SPRAY TECHNIQUE

Electrostatic spray deposition (ESD) is a technique to deposit a thin film coating upon various substrates. ESD setup utilizes the same components of the EHD system, materials and procedure except the stand-off distance. In the ESD technique, ink is pumped to the nozzle at appropriate flow rate, a high DC voltage (kV) is applied between nozzle and substrate holder. Electrostatic charge is developed between the substrate and nozzle that results generation of droplets from the nozzle. As compared to EHD process, the distance between nozzle and substrate is long (stand-off distance) that results the formation of spray from the droplets due to high electric field. In this scenario, ink is positively charged whereas the substrate is negative, positively charged ink is uniformly attracted towards the substrate. ESD setup is shown in FIGURE 13(a), main components are ink reservoir and syringe, micrometer nozzle, high voltage supply, high speed camera, a computer controlled moveable stage and PC for the overall system control. FIGURE 13(b) shows a PVP thin film deposited through ESD system. Film deposition is started from a corner of the substrate and moving the substrate at a constant speed to cover it with the material. If the substrate is large, the spray cannot complete it in one step. Usually, the spray covers almost 10 mm space on the substrate; hence next step is to start the spray at 10 mm distance from the first patch. This way the entire substrate is covered with material with single pass. The thickness of the film is controlled

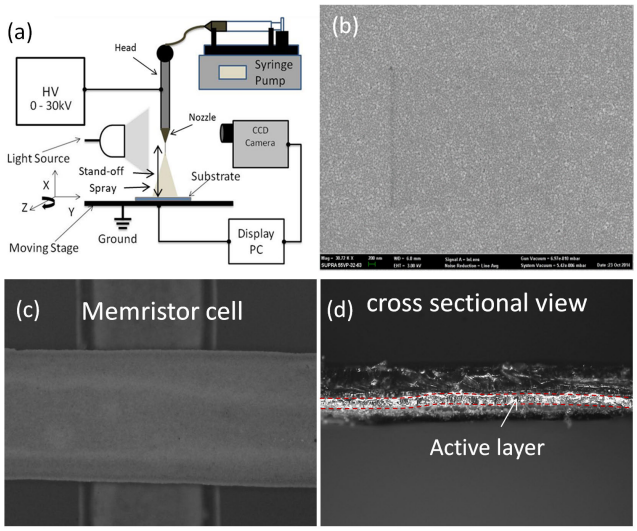

FIGURE 13. **(a) Electrostatic spray deposition setup, (b) PVP thin active layer deposited through ESD (c) memristor crossbar structure, (d) cross sectional view of memristor cell.**

through the number of depositions passes and speed of the stage that hold substrate. Number of passes can be deposited by two methods. Depositing a layer of the material and let the substrate dry before applying next layer (pass), this method is called layer by layer. The second method is to apply next pass immediately after finishing the first layer while it is still wet, this method is called blended layer deposition because the later layer can penetrate in the first layer. FIGURE 13(c) shows microscopic image of the memristor crossbar cell with transparent active layer. Bottom and top electrodes are visible whereas the active layer PVP is not visible. FIGURE 13(d) shows cross sectional view of the memristor with active layer deposited through ESD system. It can be seen the active layer is uniform and consistent throughout. ESD requires ink with low viscosity in order to make spray. Solution viscosity range is from 0.001 to 0.10 Pa.S and the surface tension of the ink is usually 15 to 25 mN/m. There are several challenges in the ESD system to deposit a uniform film, especially when the substrate is of large area. The ESD system cannot cover the entire substrate area at once; hence need the substrate to move with a uniform speed which covers almost 10 mm wide line. The substrate is covered with 10 mm lines one by one. In this procedure, some material overlaps the previous line and makes it thicker as compared to the center of the line. It is difficult to get large area nm thick film over the substrate, however, small area films i.e. memristor array can be perfectly deposit through ESD. ESD systems are usually custom made according to the requirements. ESD system can be configured in single nozzle, and multi-nozzles. ESD systems are always continuous jetting system to avoid non-uniformity of the deposited film.

VI. TOP ELECTRODES

Top electrode is the final layer of memristor structure. This layer is the most challenging because it can penetrate in the active layer in case of solution based materials as well as in thermal evaporation technique.

In printing techniques the top layer is always affected by the sandwich layer, sometimes it spreads out and sometimes shrinks down. In both cases there is possibility of open circuit of the top electrode bars. This problem happens due to sandwich layer's property, if it is hydrophilic the top electrode material spreads over and if he sandwich layer is hydrophobic, the top electrode material will shrink down. The problem can be addressed with surface treatment of the sandwich layer in such a way not to disturb the chemical properties of the layer as the sandwich layer is either insulator or metal oxide. The material printing quality mainly controlled through material's viscosity, surface tension and substrate surface energy [71], [120]. FIGURE **14**(a) shows a crossbar memory device fabricated through inkjet material printer. The device consists of PET substrate, silver bottom electrode, graphene oxide active layer, and silver top electrode. The top electrode over the active region is not uniformed; rather it is spread over the active layer. On the other hand, the silver material of top electrode on the PET substrate is uniform. This confirms the incompatibility between active layer and silver material. FIGURE **14**(b) shows a crossbar memory array on a glass substrate, consisted of silver electrodes, zinc oxide active layer, and silver top electrode. Bottom and top electrodes are not symmetrical in width, although both were deposited as 200 μm width. The top electrode material shrank down due to the active layer's mismatch with silver material and its solution. FIGURE **14**(c) shows bottom electrode bars and active layer fabricated through inkjet material printer on a PET substrate. PEDOT:PSS bottom electrodes and Zinc oxide in ethanol active layer. In this scenario, PEDOT:PSS and PET substrate's attachbility was not good and also the solution of PEDT:PSS and Zinc Oxide was not compatible,

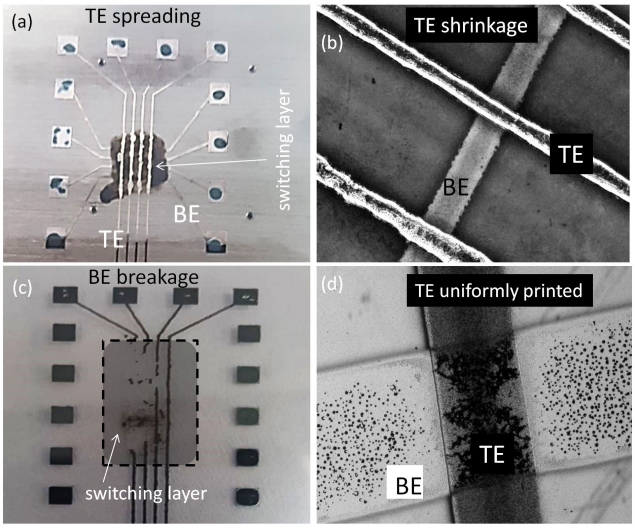

FIGURE 14. **(a) Silver TE with spreading affect, (b) silver TE with shrinkage effect, (c) BE breakage due to switching layer effect, (d) uniformly printing of TE with switching layer treated.**

as shown in FIGURE **14**(c). TABLE 1 show the available printed electronics technologies for the fabrication of memristors. For the crossbar electrodes many technologies are available which can fabricate as low as 1μm such as nanoimprint [1]–[3]. All the printed technologies offer some benefits and drawbacks over the others such as fabrication steps, material waste, specific material's viscosity and surface tension, pattern resolution and thickness, controlled environment, and printing speed. Inkjet material printer is suitable for the crossbar electrode fabrication, it offers mask less fabrication without materials waste and rapid prototyping [1]–[3]. On the other hand aerosol jet is more suitable for patterns fabrication because it provide high resolution as low as 10 μm width, high printing speed, and least material wastage [9], [11]. EHD technology can be used for the patterns fabrication in low stand-off mode in order make pattern rather than spray [5]. Stand-off distance is a distance between the nozzle and substrate. If the stand-off distance is high the jet converts into spray whereas in low stand-off distance the jet directly hit the substrate with thin tip. EHD technique is comparative complex in terms of material optimization to make a canonical jet, stand-off distance setting, and other parameters such as material flow, operating voltage and platen moving speed [6], [121]. As compared to patterns printing, active layer printing is limited to few printed techniques because the active layer requires thin films. For the thin film fabrication several techniques can be used however, the material's viscosity and surface tension need to be synthesized. The easy way to control the thickness is spin coating technique where the thickness is controlled through the operating revolution per minute rpm [17]–[20]. Screen printing technique is not suitable for the memristor fabrication because the patterns are too thick, that affect the active layer. Three steps and screens are needed to make a crossbar array i.e., bottom electrode, top electrode and active layer. Screen printer is not suitable for making the prototype of memristor crossbar array because, it is difficult to use as compared to other techniques, consumes more time in settings, changing screen, and cleaning [3], [12].

VII. SUBSTRATE SELECTION

Substrate selection is based on the memristor device application, it can be rigid, flexible, and even stretchable. Technically substrate does not affect the performance of device as long as the device layers are compatible with deformation and with mechanical properties of the substrate. However, thermal conductivity of the substrate affects the resistance of the device in both state due to rise in temperature [122]. In case of flexible device fabrication, the substrate could be plastic, paper, or thin glass. Materials used in the memristor layers should be capable of sustaining mechanical deformation such as stress and strain without affecting the electrical performance.

Remain glassy or crystalline. Above Tg temperature, materials behavior becomes rubbery. A plastic substrate property can be completely different above and below the Tg temperature. It is hard to fix the Tg value of a material, because the Tg depends strongly on the strain rate and cooling or heating rate. Hence, there cannot be fixed value for Tg for a specific material. Main problem of a plastic substrate is the lower Tg. Various plastic substrates are summarized according to their Tg in FIGURE 15. Lower Tg of the polymer substrate limits its use to organic materials only. Plastic substrates are categorized into three main classes: 1) semi-crystalline, 2) amorphous and 3) solution cast amorphous. Semi-crystalline polymers are used in flexible substrates including polyethylene napthalate (PEN), and heat stabilized PEN, polyethylene terephthalate (PET), heat stabilized (PET), and polyetheretherketone (PEEK). Amorphous polymer substrates cover Polyethersulphone (PES), and polycarbonate (PC), these materials are non-crystalline in nature which can be melt-extruded [77]. Some of the amorphous groups that cannot be melt-processed include such as polycarbonate (PC), polyarylate (PAR), Polyethersulphone (PES), polycyclic olefin (PCO), and polyimide (PI).

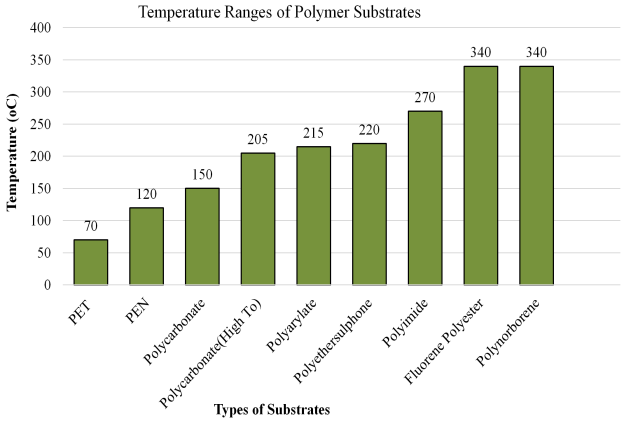

FIGURE 15. Tg of commonly used plastic substrates in printed memristors fabrication [123].

VIII. ENCAPSULATION

Encapsulation plays an important role in the device performance and life span of printed electronics [124], [125]. Especially thin film organic electronic devices are prone to water vapors and oxidation [126]. Memristors are thin film devices made up of thin patterned electrodes and thin film sandwich active layer. Both electrodes and sandwich layer can be fabricated with variety of materials including organic and inorganic [127]. Usually the sandwich layer is oxide based material which can easily be oxidized from the environment, similarly the electrodes also get oxidized with time. If the device is not encapsulated right after the fabrication, oxidation starts slowly which affects the important factor in the substrate selection is its transition temperature. Not only in the fabrication process where annealing of the device takes high temperature, but also during the device operation where the device get instantaneous variation in temperature due to current flow. The glass transition temperature of a substrate, usually called Tg, is an important property when considering

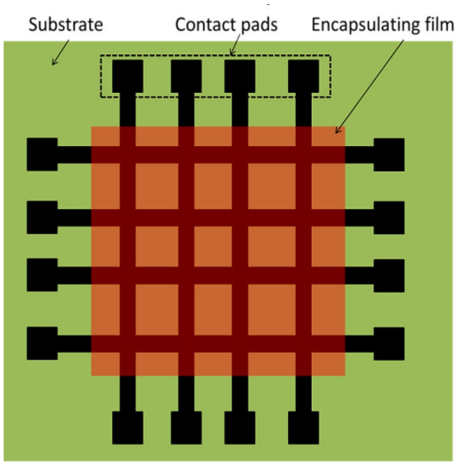

FIGURE 16. Architecture of memristor array with encapsulating layer.

polymers for a particular application. Below the Tg a plastic's molecules have relatively little mobility. Glass transition temperature is the threshold temperature of a material below which the physical properties of plastics performance of the device and life. Usually resistive devices face a problem of positive resistance variation along the time period due to oxidation. Oxidation increases the resistance of memristor in either resistive states i.e. HRS and LRS. Therefore encapsulation is very important step in the electronic devices and systems to prevent oxidation and other environmental effects such as humidity, light, and temperature. In case of memristor device, oxidation affect the state resistance value usually the resistance is increased with time. Memristor without encapsulation are prone to resistance variation and the retention time is short. Encapsulation layer can be applied on the active area of the crossbar array in such way not to cover the contact pads as shown in FIGURE 16. In this way only the input/output contact pad is exposed, and the rest of the devices are encapsulated. Variety of encapsulation methods are used to protect the device from the environmental effects, some popular and relevant to the memristor encapsulating techniques are discussed below

A. PDMS ENCAPSULATION

Printed memristors are highly prone to environmental effects and oxidation. PDMS is biocompatible and environmental friendly materials mainly used in biomedical applications. PDMS provides very good encapsulating property among its various characteristics i.e. insulator, rubber like property, easy molding, and low cost. PDMS is actively used in memristor fabrication for the encapsulating layer [128], [129]. PDMS comes with a variety of advantages such as conformability, flexibility, transparent, and strong adhesion. PDMS material comes in two parts, base and curing agent. Usually they are mixed with 10:1 (base: curing agent), followed by degasing in a chamber to remove air bubbles inside the material. Pre-polymerized PDMS is applied to the target surface and then cured at 80°C for an hour to polymerize the material. Once the PDMS is polymerized, it become a part of the device and holds the device and protects it against environmental effects such as humidity, wetting, and mechanical stress. In case of memristor array encapsulation with PDMS, the encapsulating material is applied over the crossbar structure by avoiding the contact pads as shown in FIGURE 16. The pads are not encapsulated to allow the electrical contact with measuring electronic devices such as wire bonding or probe station. In printed memristor crossbar arrays, encapsulation is very important because printed devices are fabricated at low temperatures and usually at ambient conditions. Devices without encapsulation exhibits limited endurance cycles as compared to those encapsulated ones [7], [129]–[132].

B. PDMS ENCAPSULATION

Atomic layer deposition (ALD) technique was introduced in late 1970s by Tampere University of Technology [7]. ALD got tremendous attraction as it can deposit an atom size thin film on the top of device for encapsulation [133]–[135]. The working technique of the ALD system is based on exposing the substrate to two different reactants in sequential and alternative way. These reactants reacts with the surface in self-limiting way, which controls the thickness of the encapsulating film. The self-limiting growth feature of the ALD system ensures the growth of thin film with accurate thickness on large and uneven surfaces [136], [137]. Uniform and thin films grown through ALD system are achieved by an AB binary sequential reaction, separated by washing flow of N_2 [138]. ALD offers encapsulating thin film deposition over uneven, flexible, rigid, transparent, and opaque substrates, which makes it ideal for the organic electronic fabrication. Al_2O_3 film was deposited over a memristor crossbar array for the encapsulation [139]. The device structure was $Ag/PVP/Ag/Al_2O_3$. They reported that, Al_2O_3 encapsulated memristor performed with superior stability for more than four weeks whereas the un-encapsulated devices could only last for one week. Another memristive device was presented with ALD encapsulation of 10 nm HfO_2 film at 225 °C using TDMAH and H_2O as precursors and N_2 as carrier and purge gas. The device structure was $TiN/Ti/HfO_2/W$ on a 100 mm diameter Si-n^{++} wafer [140], [141]. A1N based memristor devices were presented [142]. The devices were encapsulated with Al_2O_3, they reported the devices with encapsulating layer out performed [143].

IX. CONCLUSION

Memristor printing fabrication processes and technologies were reviewed. State of the art technologies used in the device manufacturing were reviewed for all the layers of memristor such as bottom electrode, top electrode, and active layer. Technologies for the memristor electrodes fabrication, and challenges involved in the electrode deposition such as thickness of the electrode and top electrode fabrication challenges were discussed. Selection of suitable fabrication technique for the required electrode size, and active layer thickness was discussed based on the resolution and pattern/film thickness. Substrates for the memristor crossbar

array were discussed based on the deformation, flexibility and adhesion. Encapsulation techniques i.e. ALD and standard encapsulation with PDMS and benefits of the encapsulating films were discussed.

ACKNOWLEDGMENT

The authors are thankful to Qatar National Library (QNL) for supporting the publication charges of this research article.

REFERENCES

[1] D. Tobjörk and R. Österbacka, "Paper electronics," *Adv. Mater.*, vol. 23, no. 17, pp. 1935–1961, May 2011.
[2] J. Perelaer, P. J. Smith, D. Mager, D. Soltman, S. K. Volkman, V. Subramanian, J. G. Korvink, and U. S. Schubert, "Printed electronics: The challenges involved in printing devices, interconnects, and contacts based on inorganic materials," *J. Mater. Chem.*, vol. 20, no. 39, pp. 8446–8453, 2010.
[3] J. Siden and H.-E. Nilsson, "Line width limitations of flexographic-screen- and inkjet printed RFID antennas," in *Proc. IEEE Antennas Propag. Soc. Int. Symp.*, Jun. 2007, pp. 1745–1748.
[4] S. Ali, A. Hassan, G. Hassan, J. Bae, and C. H. Lee, "Flexible frequency selective passive circuits based on memristor and capacitor," *Organic Electron.*, vol. 51, pp. 119–127, Dec. 2017.
[5] S. Ali, J. Bae, K. H. Choi, C. H. Lee, Y. H. Doh, S. Shin, and N. P. Kobayashi, "Organic non-volatile memory cell based on resistive elements through electro-hydrodynamic technique," *Organic Electron.*, vol. 17, pp. 121–128, Feb. 2015.
[6] S. Ali, J. Bae, and C. H. Lee, "Printed non-volatile resistive switches based on zinc stannate ($ZnSnO_3$)," *Current Appl. Phys.*, vol. 16, no. 7, pp. 757–762, Jul. 2016.
[7] S. Ali, J. Bae, C. H. Lee, K. H. Choi, and Y. H. Doh, "All-printed and highly stable organic resistive switching device based on graphene quantum dots and polyvinylpyrrolidone composite," *Organic Electron.*, vol. 25, pp. 225–231, Oct. 2015.
[8] M. J. Catenacci, P. F. Flowers, C. Cao, J. B. Andrews, A. D. Franklin, and B. J. Wiley, "Fully printed memristors from Cu-SiO_2 core-shell nanowire composites," *J. Electron. Mater.*, vol. 46, pp. 4596–4603, Jun. 2017.
[9] A. Mahajan, C. D. Frisbie, and L. F. Francis, "Optimization of aerosol jet printing for high-resolution, high-aspect ratio silver lines," *ACS Appl. Mater. Interfaces*, vol. 5, no. 11, pp. 4856–4864, Jun. 2013.
[10] E. Jabari and E. Toyserkani, "Micro-scale aerosol-jet printing of graphene interconnects," *Carbon*, vol. 91, pp. 321–329, Sep. 2015.
[11] E. Jabari and E. Toyserkani, "Aerosol-jet printing of highly flexible and conductive graphene/silver patterns," *Mater. Lett.*, vol. 174, pp. 40–43, Jul. 2016.
[12] R. Soukup, A. Hamáček, and J. Řeboun, "Organic based sensors: Novel screen printing technique for sensing layers deposition," in *Proc. 35th Int. Spring Seminar Electron. Technol.*, May 2012, pp. 19–24.
[13] C. W. P. Shi, X. Shan, G. Tarapata, R. Jachowicz, J. Weremczuk, and H. T. Hui, "Fabrication of wireless sensors on flexible film using screen printing and via filling," *Microsyst. Technol.*, vol. 17, no. 4, pp. 661–667, Apr. 2011.
[14] W.-Y. Chang, T.-H. Fang, H.-J. Lin, Y.-T. Shen, and Y.-C. Lin, "A large area flexible array sensors using screen printing technology," *J. Display Technol.*, vol. 5, no. 6, pp. 178–183, Jun. 2009.
[15] H. Kempa, M. Hambsch, K. Reuter, M. Stanel, G. C. Schmidt, B. Meier, and A. C. Hubler, "Complementary ring oscillator exclusively prepared by means of gravure and flexographic printing," *IEEE Trans. Electron Devices*, vol. 58, no. 8, pp. 2765–2769, Aug. 2011.
[16] P. F. Moonen, I. Yakimets, and J. Huskens, "Fabrication of transistors on flexible substrates: From mass-printing to high-resolution alternative lithography strategies," *Adv. Mater.*, vol. 24, no. 41, pp. 5526–5541, Nov. 2012.
[17] D. B. Hall, P. Underhill, and J. M. Torkelson, "Spin coating of thin and ultrathin polymer films," *Polym. Eng. Sci.*, vol. 38, no. 12, pp. 2039–2045, Dec. 1998.
[18] K. Yan, M. Peng, X. Yu, X. Cai, S. Chen, H. Hu, B. Chen, X. Gao, B. Dong, and D. Zou, "High-performance perovskite memristor based on methyl ammonium lead halides," *J. Mater. Chem. C*, vol. 4, no. 7, pp. 1375–1381, 2016.
[19] M. Nelo, M. Sloma, J. Kelloniemi, J. Puustinen, T. Saikkonen, J. Juuti, J. Häkkinen, M. Jakubowska, and H. Jantunen, "Inkjet-printed memristor: Printing process development," *Jpn. J. Appl. Phys.*, vol. 52, May 2013, Art. no. 05DB21.
[20] K. Rajan, S. Bocchini, A. Chiappone, I. Roppolo, D. Perrone, K. Bejtka, C. Ricciardi, C. F. Pirri, and A. Chiolerio, "Spin-coated silver nanocomposite resistive switching devices," *Microelectron. Eng.*, vol. 168, pp. 27–31, Jan. 2017.
[21] C.-F. Lin, B.-K. Wang, C. Tiu, and T.-J. Liu, "On the pinning of downstream meniscus for slot die coating," *Adv. Polym. Technol.*, vol. 32, no. S1, pp. E249–E257, Mar. 2013.
[22] L. Hu, H. S. Kim, J.-Y. Lee, P. Peumans, and Y. Cui, "Scalable coating and properties of transparent, flexible, silver nanowire electrodes," *ACS Nano*, vol. 4, no. 5, pp. 2955–2963, May 2010.
[23] J. Simmons and R. Verderber, "New thin-film resistive memory," *Radio Electron. Eng.*, vol. 34, no. 2, pp. 81–89, 1967.
[24] E. L. Cook, "Model for the resistive-conductive transition in reversible resistance-switching solids," *J. Appl. Phys.*, vol. 41, no. 2, pp. 551–554, Feb. 1970.
[25] T.-M. Lee, S.-H. Lee, J.-H. Noh, D.-S. Kim, and S. Chun, "The effect of shear force on ink transfer in gravure offset printing," *J. Micromech. Microeng.*, vol. 20, no. 12, Dec. 2010, Art. no. 125026.
[26] N. Choi, H. Wee, S. Nam, J. Lavelle, and M. Hatalis, "A modified offset roll printing for thin film transistor applications," *Microelectron. Eng.*, vol. 91, pp. 93–97, Mar. 2012.
[27] T.-M. Lee, J.-H. Noh, I. Kim, D.-S. Kim, and S. Chun, "Reliability of gravure offset printing under various printing conditions," *J. Appl. Phys.*, vol. 108, no. 10, Nov. 2010, Art. no. 102802.
[28] D. Sung, A. de la Fuente Vornbrock, and V. Subramanian, "Scaling and optimization of gravure-printed silver nanoparticle lines for printed electronics," *IEEE Trans. Compon. Packag. Technol.*, vol. 33, no. 1, pp. 105–114, Mar. 2010.
[29] J. Noh, K. Jung, J. Kim, S. Kim, S. Cho, and G. Cho, "Fully gravure-printed flexible full adder using SWNT-based TFTs," *IEEE Electron Device Lett.*, vol. 33, no. 11, pp. 1574–1576, Nov. 2012.
[30] H. Park, H. Kang, Y. Lee, Y. Park, J. Noh, and G. Cho, "Fully roll-to-roll gravure printed rectenna on plastic foils for wireless power transmission at 13.56 MHz," *Nanotechnology*, vol. 23, no. 34, Aug. 2012, Art. no. 344006.
[31] A. Perl, D. N. Reinhoudt, and J. Huskens, "Microcontact printing: Limitations and achievements," *Adv. Mater.*, vol. 21, no. 22, pp. 2257–2268, Jun. 2009.
[32] T. Kaufmann and B. J. Ravoo, "Stamps, inks and substrates: Polymers in microcontact printing," *Polym. Chem.*, vol. 1, no. 4, pp. 371–387, 2010.
[33] B. Li, J. Zhang, and H. Ge, "A sandwiched flexible polymer mold for control of particle-induced defects in nanoimprint lithography," *Appl. Phys. A*, vol. 110, no. 1, pp. 123–128, Jan. 2013.
[34] S. A. Ruiz and C. S. Chen, "Microcontact printing: A tool to pattern," *Soft Matter*, vol. 3, no. 2, pp. 168–177, 2007.
[35] Y. Sun and J. A. Rogers, "Inorganic semiconductors for flexible electronics," *Adv. Mater.*, vol. 19, no. 15, pp. 1897–1916, Aug. 2007.
[36] R. S. Dahiya, A. Adami, C. Collini, and L. Lorenzelli, "Fabrication of single crystal silicon micro-/nanostructures and transferring them to flexible substrates," *Microelectron. Eng.*, vol. 98, pp. 502–507, Oct. 2012.
[37] A. J. Baca, J.-H. Ahn, Y. Sun, M. A. Meitl, E. Menard, H.-S. Kim, W. M. Choi, D.-H. Kim, Y. Huang, and J. A. Rogers, "ChemInform abstract: Semiconductor wires and ribbons for high-performance flexible electronics," *ChemInform*, vol. 39, no. 43, pp. 5524–5542, Oct. 2008.
[38] L. Chua, "Memristor—The missing circuit element," *IEEE Trans. Circuit Theory*, vol. CT-18, no. 5, pp. 507–519, Sep. 1971.
[39] D. B. Strukov, G. S. Snider, D. R. Stewart, and R. S. Williams, "The missing memristor found," *Nature*, vol. 453, no. 7191, p. 80, May 2008.
[40] N. K. Upadhyay, W. Sun, P. Lin, S. Joshi, R. Midya, X. Zhang, Z. Wang, H. Jiang, J. H. Yoon, M. Rao, M. Chi, Q. Xia, and J. J. Yang, "A memristor with low switching current and voltage for 1S1R integration and array operation," *Adv. Electron. Mater.*, vol. 6, no. 5, May 2020, Art. no. 1901411.
[41] G. S. Kim, H. Song, Y. K. Lee, J. H. Kim, W. Kim, T. H. Park, H. J. Kim, K. M. Kim, and C. S. Hwang, "Defect-engineered electroforming-free analog HfO_x memristor and its application to the neural network," *ACS Appl. Mater. Interfaces*, vol. 11, pp. 47063–47072, Nov. 2019.

[42] J. P. Strachan, J. J. Yang, L. A. Montoro, C. A. Ospina, A. J. Ramirez, A. L. D. Kilcoyne, G. Medeiros-Ribeiro, and R. S. Williams, "Characterization of electroforming-free titanium dioxide memristors," *Beilstein J. Nanotechnol.*, vol. 4, pp. 467–473, Aug. 2013.

[43] T. D. Dongale, K. P. Patil, S. B. Mullani, K. V. More, S. D. Delekar, P. S. Patil, P. K. Gaikwad, and R. K. Kamat, "Investigation of process parameter variation in the memristor based resistive random access memory (RRAM): Effect of device size variations," *Mater. Sci. Semicond. Process.*, vol. 35, pp. 174–180, Jul. 2015.

[44] S. Kim, S. Jung, M.-H. Kim, Y.-C. Chen, Y.-F. Chang, K.-C. Ryoo, S. Cho, J.-H. Lee, and B.-G. Park, "Scaling effect on silicon nitride memristor with highly doped Si substrate," *Small*, vol. 14, no. 19, May 2018, Art. no. 1704062.

[45] S. Pi, C. Li, H. Jiang, W. Xia, H. Xin, J. J. Yang, and Q. Xia, "Memristor crossbar arrays with 6-nm half-pitch and 2-nm critical dimension," *Nature Nanotechnol.*, vol. 14, no. 1, pp. 35–39, Jan. 2019.

[46] S. Zou, P. Xu, and M. C. Hamilton, "Resistive switching characteristics in printed Cu/CuO/(AgO)/Ag memristors," *Electron. Lett.*, vol. 49, no. 13, pp. 829–830, Jun. 2013.

[47] S. Khan, S. Ali, and A. Bermak, "Smart manufacturing technologies for printed electronics," in *Hybrid Nanomaterials: Flexible Electronics Materials*. London, U.K.: InTech, 2019.

[48] H. Schicht, "Clean room technology: The concept of total environmental control for advanced industries," *Vacuum*, vol. 35, nos. 10–11, pp. 485–491, Oct. 1985.

[49] S. Khumpuang and S. Hara, "A MOSFET fabrication using a maskless lithography system in clean-localized environment of minimal fab," *IEEE Trans. Semicond. Manuf.*, vol. 28, no. 3, pp. 393–398, Aug. 2015.

[50] S. Paul, P. G. Harris, C. Pal, A. K. Sharma, and A. K. Ray, "Low cost zinc oxide for memristors with high on-off ratios," *Mater. Lett.*, vol. 130, pp. 40–42, Sep. 2014.

[51] B. Sharma and M. K. Rabinal, "A simple dip coat patterning of aluminum oxide to constitute a bistable memristor," *Mater. Res. Exp.*, vol. 3, no. 12, Dec. 2016, Art. no. 126302.

[52] S. Patil, M. Chougale, T. Rane, S. Khot, A. Patil, O. Bagal, S. Jadhav, A. Sheikh, S. Kim, and T. Dongale, "Solution-processable ZnO thin film memristive device for resistive random access memory application," *Electronics*, vol. 7, no. 12, p. 445, Dec. 2018.

[53] A. I. Vlasov, I. V. Gudoshnikov, V. P. Zhalnin, A. T. Kadyr, and V. A. Shakhnov, "Market for memristors and data mining memory structures for promising smart systems," *Entrepreneurship Sustainability Issues*, vol. 8, no. 2, p. 98, 2020.

[54] H. Abbas, Y. Abbas, S. N. Truong, K.-S. Min, M. R. Park, J. Cho, T.-S. Yoon, and C. J. Kang, "A memristor crossbar array of titanium oxide for non-volatile memory and neuromorphic applications," *Semicond. Sci. Technol.*, vol. 32, no. 6, Jun. 2017, Art. no. 065014.

[55] B. Salonikidou, T. Yasunori, B. Le Borgne, J. England, T. Shizuo, and R. A. Sporea, "Toward fully printed memristive elements: A-TiO_2 electronic synapse from functionalized nanoparticle ink," *ACS Appl. Electron. Mater.*, vol. 1, no. 12, pp. 2692–2700, Dec. 2019.

[56] R. M. Pasquarelli, D. S. Ginley, and R. O'Hayre, "Solution processing of transparent conductors: From flask to film," *Chem. Soc. Rev.*, vol. 40, no. 11, pp. 5406–5441, 2011.

[57] V. C. Tung, M. J. Allen, Y. Yang, and R. B. Kaner, "High-throughput solution processing of large-scale graphene," *Nature Nanotechnol.*, vol. 4, no. 1, p. 25, 2009.

[58] N. Gergel-Hackett, B. Hamadani, B. Dunlap, J. Suehle, C. Richter, C. Hacker, and D. Gundlach, "A flexible solution-processed memristor," *IEEE Electron Device Lett.*, vol. 30, no. 7, pp. 706–708, Jul. 2009.

[59] J. Ouyang, C.-W. Chu, R. J.-H. Tseng, A. Prakash, and Y. Yang, "Organic memory device fabricated through solution processing," *Proc. IEEE*, vol. 93, no. 7, pp. 1287–1296, Jul. 2005.

[60] D. Mitzi, *Solution Processing of Inorganic Materials*. Hoboken, NJ, USA: Wiley, 2008.

[61] L. I. N. Tomé, V. Baião, W. da Silva, and C. M. A. Brett, "Deep eutectic solvents for the production and application of new materials," *Appl. Mater. Today*, vol. 10, pp. 30–50, Mar. 2018.

[62] F. M. Kerton and R. Marriott, *Alternative Solvents for Green Chemistry*. London, U.K.: Royal Society of Chemistry, 2013.

[63] S. Ali, S. Khan, and A. Bermak, "Inkjet-printed human body temperature sensor for wearable electronics," *IEEE Access*, vol. 7, pp. 163981–163987, 2019.

[64] S. A. Hadi, K. M. Humood, M. A. Jaoude, H. Abunahla, H. F. A. Shehhi, and B. Mohammad, "Bipolar Cu/HfO_2/p^{++} Si memristors by sol-gel spin coating method and their application to environmental sensing," *Sci. Rep.*, vol. 9, no. 1, pp. 1–15, Dec. 2019.

[65] H. A. O. Hill, I. J. Higgins, J. M. McCann, and G. Davis, "Strip electrode with screen printing," U.S. Patent 5 820 551 A, Oct. 13, 1998.

[66] C. J. Brinker, G. C. Frye, A. J. Hurd, and C. S. Ashley, "Fundamentals of sol-gel dip coating," *Thin Solid Films*, vol. 201, no. 1, pp. 97–108, Jun. 1991.

[67] D. R. Elvidge and M. K. Smith, "Metering rod coaters," U.S. Patent 5 599 393 A, Feb. 4, 1997.

[68] A. Mette, P. L. Richter, M. Hörteis, and S. W. Glunz, "Metal aerosol jet printing for solar cell metallization," *Prog. Photovolt., Res. Appl.*, vol. 15, no. 7, pp. 621–627, 2007.

[69] H. Yang and P. Jiang, "Large-scale colloidal self-assembly by doctor blade coating," *Langmuir*, vol. 26, no. 16, pp. 13173–13182, Aug. 2010.

[70] E. Gale, B. de Lacy Costello, and A. Adamatzky, "The effect of electrode size on memristor properties: An experimental and theoretical study," in *Proc. IEEE Int. Conf. Electron. Design, Syst. Appl. (ICEDSA)*, Nov. 2012, pp. 80–85.

[71] S. Krainer, C. Smit, and U. Hirn, "The effect of viscosity and surface tension on inkjet printed picoliter dots," *RSC Adv.*, vol. 9, no. 54, pp. 31708–31719, 2019.

[72] K. Nagashima, T. Yanagida, M. Kanai, K. Oka, A. Klamchuen, S. Rahong, G. Meng, M. Horprathum, B. Xu, F. Zhuge, Y. He, and T. Kawai, "Switching properties of titanium dioxide nanowire memristor," *Jpn. J. Appl. Phys.*, vol. 51, no. 11, 2012, Art. no. 11PE09.

[73] H.-C. Wu and H.-J. Lin, "Effects of actuating pressure waveforms on the droplet behavior in a piezoelectric inkjet," *Mater. Trans.*, vol. 51, no. 12, Dec. 2010, Art. no. 1011151219.

[74] H.-J. Lin, H.-C. Wu, T.-R. Shan, and W.-S. Hwang, "The effects of operating parameters on micro-droplet formation in a piezoelectric inkjet printhead using a double pulse voltage pattern," *Mater. Trans.*, vol. 47, no. 2, pp. 375–382, 2006.

[75] A. Hassan, S. Ali, G. Hassan, J. Bae, and C. H. Lee, "Inkjet-printed antenna on thin PET substrate for dual band Wi-Fi communications," *Microsyst. Technol.*, vol. 23, no. 8, pp. 3701–3709, Aug. 2017.

[76] K. J. Yoon, J.-W. Han, D.-I. Moon, M. L. Seol, M. Meyyappan, H. J. Kim, and C. S. Hwang, "Electrically-generated memristor based on inkjet printed silver nanoparticles," *Nanosc. Adv.*, vol. 1, no. 8, pp. 2990–2998, 2019.

[77] S. Porro and C. Ricciardi, "Memristive behaviour in inkjet printed graphene oxide thin layers," *RSC Adv.*, vol. 5, no. 84, pp. 68565–68570, 2015.

[78] G. A. Illarionov, D. S. Kolchanov, O. A. Kuchur, M. V. Zhukov, E. Sergeeva, V. V. Krishtop, A. V. Vinogradov, and M. I. Morozov, "Inkjet assisted fabrication of planar biocompatible memristors," *RSC Adv.*, vol. 9, no. 62, pp. 35998–36004, 2019.

[79] S. Khan and D. Briand, "Fabrication techniques for coupling advanced nanomaterials to transducers," in *Advanced Nanomaterials for Inexpensive Gas Microsensors*. Amsterdam, The Netherlands: Elsevier, 2020, pp. 103–124.

[80] S. Khan, T. P. Nguyen, M. Lubej, L. Thiery, P. Vairac, and D. Briand, "Low-power printed micro-hotplates through aerosol jetting of gold on thin polyimide membranes," *Microelectron. Eng.*, vol. 194, pp. 71–78, Jul. 2018.

[81] S. Khan and D. Briand, "All-printed low-power metal oxide gas sensors on polymeric substrates," *Flexible Printed Electron.*, vol. 4, no. 1, Feb. 2019, Art. no. 015002.

[82] S. Li, J. G. Park, S. Wang, R. Liang, C. Zhang, and B. Wang, "Working mechanisms of strain sensors utilizing aligned carbon nanotube network and aerosol jet printed electrodes," *Carbon*, vol. 73, pp. 303–309, Jul. 2014.

[83] X. Feng, Y. Li, L. Wang, S. Chen, Z. G. Yu, W. C. Tan, N. Macadam, G. Hu, L. Huang, L. Chen, X. Gong, D. Chi, T. Hasan, A. V. Thean, Y. Zhang, and K. Ang, "A fully printed flexible MoS_2 memristive artificial synapse with femtojoule switching energy," *Adv. Electron. Mater.*, vol. 5, no. 12, Dec. 2019, Art. no. 1900740.

[84] P. Vilmi, M. Nelo, J.-V. Voutilainen, J. Palosaari, J. Pörhönen, S. Tuukkanen, H. Jantunen, J. Juuti, and T. Fabritius, "Fully printed memristors for a self-sustainable recorder of mechanical energy," *Flexible Printed Electron.*, vol. 1, no. 2, Jun. 2016, Art. no. 025002.

[85] T. H. Phung, S. Oh, and K.-S. Kwon, "High-resolution patterning using two modes of electrohydrodynamic jet: Drop on demand and near-field electrospinning," *J. Visualized Exp.*, no. 137, Jul. 2018.
[86] R. R. Søndergaard, M. Hösel, and F. C. Krebs, "Roll-to-roll fabrication of large area functional organic materials," *J. Polym. Sci. B, Polym. Phys.*, vol. 51, no. 1, pp. 16–34, Jan. 2013.
[87] D. Tobjörk and R. Österbacka, "Paper electronics," *Adv. Matr.*, vol. 23, no. 17, pp. 1935–1961, 2011.
[88] R. Turunen, D. Numakura, M. Nakayama, and H. Kawasaki, "Screen printing process for high density flexible electronics," in *Proc. IPC Printed Circuit Expo/APEX* 2008, pp. 44–49.
[89] F. C. Krebs, M. Jørgensen, K. Norrman, O. Hagemann, J. Alstrup, T. D. Nielsen, J. Fyenbo, K. Larsen, and J. Kristensen, "A complete process for production of flexible large area polymer solar cells entirely using screen printing—First public demonstration," *Sol. Energy Mater. Sol. Cells*, vol. 93, no. 4, pp. 422–441, Apr. 2009.
[90] Y. J. Kwack and W. S. Choi, "Screen-printed source-drain electrodes for a solution-processed zinc-tin-oxide thin-film transistor," *J. Korean Phys. Soc.*, vol. 59, no. 6, p. 3410, 2011.
[91] W.-Y. Chang, T.-H. Fang, S.-H. Yeh, and Y.-C. Lin, "Flexible electronics sensors for tactile multi-touching," *Sensors*, vol. 9, no. 2, pp. 1188–1203, Feb. 2009.
[92] D. A. Clark, "Major trends in gravure printed electronics," California Polytech. State Univ., San Luis Obispo, CA, USA, Tech. Rep. 26, 2010. [Online]. Available: https://digitalcommons.calpoly.edu/grcsp/26
[93] G. E. Jabbour, R. Radspinner, and N. Peyghambarian, "Screen printing for the fabrication of organic light-emitting devices," *IEEE J. Sel. Topics Quantum Electron.*, vol. 7, no. 5, pp. 769–773, Sep. 2001.
[94] T. R. de Oliveira, W. T. Fonseca, G. de Oliveira Setti, and R. C. Faria, "Fast and flexible strategy to produce electrochemical paper-based analytical devices using a craft cutter printer to create wax barrier and screen-printed electrodes," *Talanta*, vol. 195, pp. 480–489, Apr. 2019.
[95] M. Aoki, K. Nakamura, T. Tachibana, I. Sumita, H. Hayashi, H. Asada, and Y. Ohshita, "30 μm fine-line printing for solar cells," in *Proc. IEEE 39th Photovolt. Spec. Conf. (PVSC)*, Jun. 2013, pp. 2162–2166.
[96] V. Subramanian, D. Soltman, S. K. Volkman, Q. Zhang, J. B. Chang, A. de la Fuente Vornbrock, D. C. Huang, L. Jagannathan, F. Liao, B. Mattis, S. Molesa, and D. R. Redinger, "Printed electronics for low-cost electronic systems: Technology status and application development," in *Proc. 38th Eur. Solid-State Device Res. Conf. (ESSDERC)*, Sep. 2008, pp. 17–24.
[97] M. Pudas, N. Halonen, P. Granat, and J. Vähäkangas, "Gravure printing of conductive particulate polymer inks on flexible substrates," *Prog. Organic Coat.*, vol. 54, no. 4, pp. 310–316, Dec. 2005.
[98] J. Yang, D. Vak, N. Clark, J. Subbiah, W. W. H. Wong, D. J. Jones, S. E. Watkins, and G. Wilson, "Organic photovoltaic modules fabricated by an industrial gravure printing proofer," *Sol. Energy Mater. Sol. Cells*, vol. 109, pp. 47–55, Feb. 2013.
[99] H. W. Kang, H. J. Sung, T.-M. Lee, D.-S. Kim, and C.-J. Kim, "Liquid transfer between two separating plates for micro-gravure-offset printing," *J. Micromech. Microeng.*, vol. 19, no. 1, Jan. 2009, Art. no. 015025.
[100] J. D. Park, S. Lim, and H. Kim, "Patterned silver nanowires using the gravure printing process for flexible applications," *Thin Solid Films*, vol. 586, pp. 70–75, Jul. 2015.
[101] Y. Kusaka, T. Kawamura, M. Nakagawa, K. Okamoto, K. Tanaka, and N. Fukuda, "Fabrication of extremely conductive high-aspect silver traces buried in hot-embossed polycarbonate films via the direct gravure doctoring method," *Adv. Powder Technol.*, vol. 32, no. 3, pp. 764–770, Mar. 2021.
[102] S. Thibert, D. Chaussy, D. Beneventi, N. Reverdy-Bruas, J. Jourdan, B. Bechevet, and S. Mialon, "Silver ink experiments for silicon solar cell metallization by flexographic process," in *Proc. 38th IEEE Photovolt. Spec. Conf.*, Jun. 2012, pp. 2266–2270.
[103] D. Deganello, J. A. Cherry, D. T. Gethin, and T. C. Claypole, "Patterning of micro-scale conductive networks using reel-to-reel flexographic printing," *Thin Solid Films*, vol. 518, no. 21, pp. 6113–6116, Aug. 2010.
[104] D. Deganello, J. A. Cherry, D. T. Gethin, and T. C. Claypole, "Impact of metered ink volume on reel-to-reel flexographic printed conductive networks for enhanced thin film conductivity," *Thin Solid Films*, vol. 520, no. 6, pp. 2233–2237, Jan. 2012.
[105] M. I. Maksud, M. S. Yusof, A. Jamil, and M. Mahadi, "A study on printed multiple solid line by combining microcontact and flexographic printing process for microelectronic and biomedical applications," *Int. J. Integr. Eng.*, vol. 5, no. 3, pp. 1–4, 2014.
[106] D. Deganello, J. A. Cherry, D. T. Gethin, and T. C. Claypole, "Patterning of micro-scale conductive networks using reel-to-reel flexographic printing," *Thin Solid Films*, vol. 518, no. 21, pp. 6113–6116, Aug. 2010.
[107] D. Deganello, J. A. Cherry, D. T. Gethin, and T. C. Claypole, "Impact of metered ink volume on reel-to-reel flexographic printed conductive networks for enhanced thin film conductivity," *Thin Solid Films*, vol. 520, no. 6, pp. 2233–2237, Jan. 2012.
[108] H. Yan, Z. Chen, Y. Zheng, C. Newman, J. R. Quinn, F. Dötz, M. Kastler, and A. Facchetti, "A high-mobility electron-transporting polymer for printed transistors," *Nature*, vol. 457, no. 7230, pp. 679–686, Feb. 2009.
[109] B. Michel, A. Bernard, A. Bietsch, E. Delamarche, M. Geissler, D. Juncker, H. Kind, J.-P. Renault, H. Rothuizen, H. Schmid, P. Schmidt-Winkel, R. Stutz, and H. Wolf, "Printing meets lithography: Soft approaches to high-resolution patterning," *IBM J. Res. Develop.*, vol. 45, no. 5, pp. 697–719, Sep. 2001.
[110] P. Kim, K. W. Kwon, M. C. Park, S. H. Lee, S. M. Kim, and S. Y. Suh, "Soft lithography for microfluidics: A review," *Biochip J.*, vol. 2, no. 1, pp. 1–11, 2008.
[111] J. A. Rogers and R. G. Nuzzo, "Recent progress in soft lithography," *Mater. Today*, vol. 8, no. 2, pp. 50–56, Feb. 2005.
[112] P. Kim, K. W. Kwon, M. C. Park, S. H. Lee, S. M. Kim, and K. Y. Suh, "Soft lithography for microfluidics: A review," Seoul Nat. Univ., Seoul, South Korea, Tech. Rep., 2008.
[113] T. Prodromakis, K. Michelakis, and C. Toumazou, "Fabrication and electrical characteristics of memristors with TiO_2/TiO_{2+x} active layers," in *Proc. IEEE Int. Symp. Circuits Syst.*, May 2010, pp. 1520–1522.
[114] S. K. Hong, J. E. Kim, S. O. Kim, S.-Y. Choi, and B. J. Cho, "Flexible resistive switching memory device based on graphene oxide," *IEEE Electron Device Lett.*, vol. 31, no. 9, pp. 1005–1007, Sep. 2010.
[115] M. S. Choi, G.-H. Lee, Y.-J. Yu, D.-Y. Lee, S. H. Lee, P. Kim, J. Hone, and W. J. Yoo, "Controlled charge trapping by molybdenum disulphide and graphene in ultrathin heterostructured memory devices," *Nature Commun.*, vol. 4, no. 1, pp. 1–7, Jun. 2013.
[116] Y.-C. King, T.-J. King, and C. Hu, "Charge-trap memory device fabricated by oxidation of $Si_{1-x}Ge_x$," *IEEE Trans. Electron Devices*, vol. 48, no. 4, pp. 696–700, Apr. 2001.
[117] M. Al-Shedivat, R. Naous, G. Cauwenberghs, and K. N. Salama, "Memristors empower spiking neurons with stochasticity," *IEEE J. Emerg. Sel. Topics Circuits Syst.*, vol. 5, no. 2, pp. 242–253, Jun. 2015.
[118] E. Solan and K. Ochs, "Wave digital emulation of general memristors," *Int. J. Circuit Theory Appl.*, vol. 46, no. 11, pp. 2011–2027, Nov. 2018.
[119] Z. Shen, C. Zhao, T. Zhao, W. Xu, Y. Liu, Y. Qi, I. Z. Mitrovic, L. Yang, and C. Z. Zhao, "Artificial synaptic performance with learning behavior for memristor fabricated with stacked solution-processed switching layers," *ACS Appl. Electron. Mater.*, vol. 3, no. 3, pp. 1288–1300, Mar. 2021.
[120] B. Derby, "Inkjet printing of functional and structural materials: Fluid property requirements, feature stability, and resolution," *Annu. Rev. Mater. Res.*, vol. 40, no. 1, pp. 395–414, Jun. 2010.
[121] S. Ali, J. Bae, and C. H. Lee, "Design of versatile printed organic resistor based on resistivity (ρ) control," *Appl. Phys. A, Solids Surf.*, vol. 119, no. 4, pp. 1499–1506, Jun. 2015.
[122] P. Basnet, D. G. Pahinkar, M. P. West, C. J. Perini, S. Graham, and E. M. Vogel, "Substrate dependent resistive switching in amorphous-HfO_x memristors: An experimental and computational investigation," *J. Mater. Chem. C*, vol. 8, no. 15, pp. 5092–5101, 2020.
[123] S. Khan, L. Lorenzelli, and R. S. Dahiya, "Technologies for printing sensors and electronics over large flexible substrates: A review," *IEEE Sensors J.*, vol. 15, no. 6, pp. 3164–3185, Jun. 2015.
[124] J.-S. Park, H. Chae, H. K. Chung, and S. I. Lee, "Thin film encapsulation for flexible AM-OLED: A review," *Semicond. Sci. Technol.*, vol. 26, no. 3, Mar. 2011, Art. no. 034001.
[125] J. Ahmad, K. Bazaka, L. J. Anderson, R. D. White, and M. V. Jacob, "Materials and methods for encapsulation of OPV: A review," *Renew. Sustain. Energy Rev.*, vol. 27, pp. 104–117, Nov. 2013.
[126] D. Yu, Y.-Q. Yang, Z. Chen, Y. Tao, and Y.-F. Liu, "Recent progress on thin-film encapsulation technologies for organic electronic devices," *Opt. Commun.*, vol. 362, pp. 43–49, Mar. 2016.
[127] R. E. Pino, J. W. Bohl, N. McDonald, B. Wysocki, P. Rozwood, K. A. Campbell, A. Oblea, and A. Timilsina, "Compact method for modeling and simulation of memristor devices: Ion conductor chalcogenide-based memristor devices," in *Proc. IEEE/ACM Int. Symp. Nanosc. Archit.*, Jun. 2010, pp. 1–4.
[128] S. Ali, J. Bae, C. H. Lee, S. Shin, and N. P. Kobayashi, "Ultra-low power non-volatile resistive crossbar memory based on pull up resistors," *Organic Electron.*, vol. 41, pp. 73–78, Feb. 2017.

[129] A. Mishra, S. Saha, H. S. Devi, A. Dixit, and M. Singh, "High resistive state retention in room temperature solution processed biocompatible memory devices for health monitoring applications," *MRS Adv.*, vol. 4, no. 24, pp. 1409–1415, May 2019.
[130] J. H. Choi, M. G. Shin, Y. Jung, D. H. Kim, and J. S. Ko, "Fabrication and performance evaluation of highly sensitive flexible strain sensors with aligned silver nanowires," *Micromachines*, vol. 11, no. 2, p. 156, Jan. 2020.
[131] S. Yuvaraja, A. Nawaz, Q. Liu, D. Dubal, S. G. Surya, K. N. Salama, and P. Sonar, "Organic field-effect transistor-based flexible sensors," *Chem. Soc. Rev.*, vol. 49, no. 11, pp. 3423–3460, 2020.
[132] L. E. Helseth, "Interdigitated electrodes based on liquid metal encapsulated in elastomer as capacitive sensors and triboelectric nanogenerators," *Nano Energy*, vol. 50, pp. 266–272, Aug. 2018.
[133] J. Meyer, A. D. Schneidenbach, T. Winkler, S. Hamwi, T. Weimann, P. Hinze, S. Ammermann, H.-H. Johannes, T. Riedl, and A. W. Kowalsky, "Reliable thin film encapsulation for organic light emitting diodes grown by low-temperature atomic layer deposition," *Appl. Phys. Lett.*, vol. 94, p. 157, Jun. 2009.
[134] L. H. Kim, K. Kim, S. Park, Y. J. Jeong, H. Kim, D. S. Chung, S. H. Kim, and C. E. Park, "Al_2O_3/TiO_2 nanolaminate thin film encapsulation for organic thin film transistors via plasma-enhanced atomic layer deposition," *ACS Appl. Mater. Interfaces*, vol. 6, no. 9, pp. 6731–6738, May 2014.
[135] S.-W. Seo, E. Jung, H. Chae, and S. M. Cho, "Optimization of Al_2O_3/ZrO_2 nanolaminate structure for thin-film encapsulation of OLEDs," *Organic Electron.*, vol. 13, no. 11, pp. 2436–2441, Nov. 2012.
[136] Y.-Q. Yang, Y. Duan, P. Chen, F.-B. Sun, Y.-H. Duan, X. Wang, and D. Yang, "Realization of thin film encapsulation by atomic layer deposition of Al_2O_3 at low temperature," *J. Phys. Chem. C*, vol. 117, no. 39, pp. 20308–20312, Oct. 2013.
[137] Y. C. Han, E. G. Jeong, H. Kim, S. Kwon, H.-G. Im, B.-S. Bae, and K. C. Choi, "Reliable thin-film encapsulation of flexible OLEDs and enhancing their bending characteristics through mechanical analysis," *RSC Adv.*, vol. 6, no. 47, pp. 40835–40843, 2016.
[138] R. W. Johnson, A. Hultqvist, and S. F. Bent, "A brief review of atomic layer deposition: From fundamentals to applications," *Mater. Today*, vol. 17, no. 5, pp. 236–246, Jun. 2014.
[139] K. Ali, J. Ali, S. M. Mehdi, K.-H. Choi, and Y. J. An, "Rapid fabrication of Al_2O_3 encapsulations for organic electronic devices," *Appl. Surf. Sci.*, vol. 353, pp. 1186–1194, Oct. 2015.
[140] S. Poblador, M. Maestro-Izquierdo, M. Zabala, M. B. González, and F. Campabadal, "Methodology for the characterization and observation of filamentary spots in HfO_x-based memristor devices," *Microelectron. Eng.*, vol. 223, Feb. 2020, Art. no. 111232.
[141] Z. Wang, D. Nminibapiel, P. Shrestha, J. Liu, W. Guo, P. G. Weidler, H. Baumgart, C. Wöll, and E. Redel, "Resistive switching nanodevices based on metal-organic frameworks," *ChemNanoMat*, vol. 2, no. 1, pp. 67–73, Jan. 2016.
[142] H. J. Yun and B. J. Choi, "Effects of moisture and electrode material on AlN-based resistive random access memory," *Ceram. Int.*, vol. 45, no. 13, pp. 16311–16316, Sep. 2019.
[143] S. Aussen, A. Hardtdegen, R. Dittmann, and S. Hoffmann-Eifert, "Memristive devices formed by ALD metal oxide growth on a hafnium layer—Study of the interfacial HfO_2 formation," in *Proc. ECS Meeting Abstr.*, 2019, p. 1232.

SHAWKAT ALI received the master's degree from the National University of Computer and Emerging Sciences, Islamabad, Pakistan, in 2012, and the Ph.D. degree in electrical/electronic engineering from Jeju National University, South Korea, in 2016. From 2016 to 2017, he was serving as an Assistant Professor with the Department of Electrical Engineering, National University of Computer and Emerging Sciences (FAST NUCES), Islamabad. Since 2017, he has been a Postdoctoral Fellow with Hamad Bin Khalifa University, Qatar. He has been involved in research throughout of his professional carrier and published more than 50 research articles, and he holds registered 13 patents and graduated three master's students. His areas of interests include radio frequency electronics, nanotechnology, wearable and implantable electronics, biomedical sensors, resistive memory, and energy harvesting. He has been awarded two times as Productive Scientist and Young Scientist by Pakistan Council for Science and Technology (PCST 2016–2018).

SALEEM KHAN received the master's degree in electronic engineering from Jeju National University, South Korea, and the Ph.D. degree in materials science engineering from the University of Trento, Italy. He worked as a Scientific Collaborator at EPFL, Switzerland, and he is currently a Postdoctoral Fellow at HBKU, Qatar Foundation, Qatar. He has more than nine years of experience in exploring printable materials and printing technologies. He also worked on the heterogeneous integration of printing and microfabrication technologies for establishing a single fabrication platform. He has contributed in more than 40 research articles and a book chapter on nanomaterials based printed gas sensors, and he holds two patents. His research activities are focused on the development of all-printed microelectronic transducers and sensing devices on polymeric substrates. He was a recipient of various prestigious scholarships like the Brain Korea 21st Century Awards Program (BK21), the Marie Curie, the Early Stage Researcher Award, and the ERC Fellow Award.

ARSHAD KHAN received the Ph.D. degree in mechanical engineering from The University of Hong Kong and the master's degree in mechatronic engineering from Jeju National University. He is currently a Postdoctoral Researcher with the College of Science and Engineering, Hamad Bin Khalifa University, Qatar Foundation. Previously, he was a joint Postdoctoral Research Fellow with the Max Planck Institute for Informatics (MPI-Inf) and the Leibniz Institute for New Materials (Leibniz-INM). His current research interests include the development of self-powered, soft wearable electronics for human activities, and health monitoring.

AMINE BERMAK (Fellow IEEE) received the master's and Ph.D. degrees in electrical and electronic engineering from Paul Sabatier University, France, in 1994 and 1998, respectively. He has held various positions in academia and industry in France, U.K., Australia, and Hong Kong. He is currently a Professor with the Information and Computing Technology Division, Hamad Bin Khalifa University. He has published over 250 articles, designed over 40 chips, and graduated 14 Ph.D. and 16 M.Phil. students. For his excellence and outstanding contribution to teaching, he was nominated for the 2013 Hong Kong UGC Best Teacher Award (for all HK Universities). He was a recipient of the 2011 University Michael G. Gale Medal for Distinguished Teaching. He was also a two-time recipient of the Engineering Teaching Excellence Award at HKUST, in 2004 and 2009, respectively. He has received six distinguished awards, including the Best University Design Contest Award at ASP-DAC 2016, the Best Paper Award at IEEE ISCAS 2010, the 2004 IEEE Chester Sall Award, and the Best Paper Award at the 2005 International Workshop on SOC for Real-Time Applications. He has served on many editorial boards and he is currently an Editor of IEEE TRANSACTIONS ON BIOMEDICAL CIRCUITS AND SYSTEMS (BioCAS) and the IEEE TRANSACTIONS ON ELECTRON DEVICES. He is a Distinguished Lecturer of IEEE.